



Department of Energy

Nevada Operations Office
P. O. Box 98518
Las Vegas, NV 89193-8518

WBS 1.2.5
QA: N/A

JAN 26 1990

King Stablein, Senior Project Manager
Repository, Licensing & Quality Assurance
Project Directorate
Division of High-Level Waste Management
U.S. Nuclear Regulatory Commission
Washington, DC 20555

U.S. NUCLEAR REGULATORY COMMISSION/U.S. DEPARTMENT OF ENERGY CALCITE-SILICA VEIN
DEPOSITS TECHNICAL EXCHANGE, FEBRUARY 6-7, 1990

References: See page 2

During the teleconference on January 16, 1990, you requested references pertaining to the forthcoming Calcite-Silica Vein Deposits Technical Exchange that were not included in the Site Characterization Plan or Study 8.3.1.5.2.1, "Characterization of the Yucca Mountain Quaternary Regional Hydrology." In response to your request, I have enclosed the references.

If you have any questions regarding these or other references pertaining to this technical exchange, please contact Ardyth M. Simmons of my staff at (702) 794-7588 or FTS 544-7588.

Carl P. Gertz, Project Manager
Yucca Mountain Project Office

YMP:AMS-1667

Enclosures:

1. U.S. Geological Survey (USGS)
Bulletin 1790, Ch. 11
2. USGS Open File Report 85-224
3. USGS Open File Report 78-701
4. USGS Bulletin 1790, Ch. 13

cc w/encls:

Steven Rossi, HQ (RW-331) FORS
C. H. Johnson, NWFO, Carson City, NV

cc w/o encls:

Gordon Appel, HQ (RW-331) FORS
J. K. Kimball, HQ (RW-221) FORS
M. A. Glora, SAIC, Las Vegas, NV
A. R. Jennetta, SAIC, Las Vegas, NV
C. L. Biddison, SAIC, Las Vegas, NV
J. L. King, SAIC, Las Vegas, NV

9002010437 900126
FDR WASTE
WM-11

PDC

FULL TEXT ASCII SCAN

102
WM-11
NH03

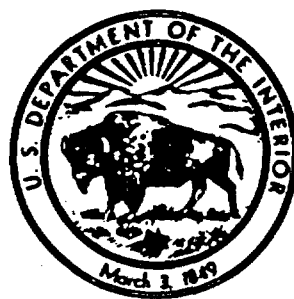
REFERENCES

- Rosholt, J. N., Swadley, W. C., and Bush, C. A., 1988, Uranium-trend dating of fluvial and fan deposits in the Beatty area, Nevada, in Carr, M. D., and Yount, J. C., eds., Geologic and Hydrologic Investigations of a Potential Nuclear Waste Disposal Site at Yucca Mountain, Southern Nevada: U.S. Geological Survey Bull. 1790, 152 pp.
- Szabo, B. J. and Kyser, T. K., 1985, Uranium, thorium isotopic analyses and uranium-series ages of calcite and opal, and stable isotopic compositions of calcite from drill cores UE25a#1, USW G-2 and USW G-3/GU-3, Yucca Mountain, Nevada: U.S. Geological Survey Open File Report OFR-85-224, 25 p.
- Szabo, B. J., and Sterr, H., 1978, Dating caliches from southern Nevada by $^{230}\text{Th}/^{232}\text{Th}$ versus $^{234}\text{U}/^{232}\text{Th}$ and $^{234}\text{U}/^{232}\text{Th}$ versus $^{238}\text{U}/^{232}\text{Th}$ isochron-plot method, in Zartman, R. E., ed., Short Papers of the Fourth International Conference, Geochronology, Cosmochronology, Isotope Geology: U.S. Geological Survey Open-File Report 78-701, p. 416-418.
- Winograd, I. J., and Szabo, B. J., 1988, Water-table decline in the south-central Great Basin during the Quaternary: implications for toxic waste disposal, in Carr, M.D., and Yount, J.C., eds., Geologic and Hydrologic Investigations of a Potential Nuclear Waste Disposal Site at Yucca Mountain, Southern Nevada: U.S. Geological Survey Bull. 1790, 152 pp.

Geological and Biological Survey
of the
of the
of the

U.S. GEOLOGICAL SURVEY BULLETIN 1790

1 (title page)



1. Introduction
By Michael D. Carr and James C. Yount
2. Regional geologic and geophysical maps of the southern Great Basin 3
By Thomas G. Hildenbrand, Albert M. Rogers, Howard W. Oliver, Stephen C. Harmsen, John K. Nakata, Douglas S. Aitken, Robert N. Harris, and Michael D. Carr
3. Preliminary interpretation of seismic-refraction and gravity studies west of Yucca Mountain, Nevada and California 23
By Hans D. Ackermann, Walter D. Mooney, David B. Snyder, and Vickie D. Sutton
4. Volcano-tectonic setting of Yucca Mountain and Crater Flat, southwestern Nevada 35
By Wilfred J. Carr
5. Detachment faulting in the Death Valley region, California and Nevada 51
By Warren B. Hamilton
6. Stress field at Yucca Mountain, Nevada 87
By Joann M. Stock and John H. Healy
7. An evaluation of the topographic modification of stresses at Yucca Mountain, Nevada 95
By Henri S. Swolfs, William Z. Savage, and William L. Ellis
8. Preliminary study of Quaternary faulting on the east side of Bare Mountain, Nye County, Nevada 103
By Marith C. Reheis
9. Reinterpretation of the Beatty scarp, Nye County, Nevada 113
By W C Swadley, James C. Yount, and Samuel T. Harding
10. Preliminary results of high-resolution seismic-reflection surveys conducted across the Beatty and Crater Flat fault scarps, Nevada 121
By Samuel T. Harding
- ⑪ Uranium-trend dating of fluvial and fan deposits in the Beatty area, Nevada 129
By John N. Rosholt, W C Swadley, and Charles A. Bush
12. Relation between *P*-wave velocity and stratigraphy of late Cenozoic deposits of southern Nevada 139
By Eduardo A. Rodriguez and James C. Yount
- ⑬ Water-table decline in the south-central Great Basin during the Quaternary: implications for toxic waste disposal 147
By Isaac J. Winograd and Barney J. Szabo

Any use of trade names is for descriptive purposes only and does not imply endorsement by the U.S. Geological Survey.

1.1. Uranium-Trend Dating of Fluvial and Fan Deposits in the Beatty Area, Nevada

By John N. Rosholt, W C Swadley, and Charles A. Bush

CONTENTS

Abstract	129
Introduction	129
Acknowledgments	130
Sample collection, preparation, and chemical procedures	131
Sample sites	131
Results	131
Discussion	132
Conclusions	136
References cited	137

Abstract

The uranium-trend dating method is used to estimate the ages of Quaternary deposits to help evaluate the age and origin of a scarp in the Beatty, Nevada, area. For dating deposits of 5 to 800 ka (thousand years) age, the open-system technique consists of determining a linear trend from analyses of six to eight channel samples collected at different depths in a depositional unit. The analytical results plotted as activity ratios of $(^{238}\text{U}-^{230}\text{Th})/^{238}\text{U}$ versus $(^{234}\text{U}-^{238}\text{U})/^{238}\text{U}$ are required for the empirical model. Ideally these data points yield a linear array in which the slope of the line of best fit changes predictably for increasingly older deposits. Analyses of deposits of known age are required to calibrate the empirical model; calibrations were provided by correlations with deposits dated by independent radiometric methods.

A sequence of the fluvial deposits next to the scarp and exposed in trench 8F-1 were sampled for dating. An age of 75 ± 15 ka was obtained for the alluvial unit of sandy silt; an underlying gravel unit indicated an age of 155 ± 25 ka and an average age of 500 ± 60 ka was obtained for three different lithologic units in lower silt and gravel deposits. Four suites of samples representing the lower silt and gravel deposits provided the following ages: clayey silt, 480 ± 50 ka; pebble gravel, 530 ± 70 ka; pebble cobble gravels, 540 ± 100 ka and 460 ± 90 ka. For the older units, the dating method does not provide sufficient resolution to distinguish differences in ages for the deposits in the 500 ka group. Disseminated carbonized wood fragments occur in the clayey silt; a radiocarbon age of $10,000 \pm 300$ yr for this wood is not consistent with the estimated 480 ka uranium-trend age of the clayey silt host-sediment.

Two separate suites representing the alluvial fan deposit that was truncated by the Beatty scarp adjacent to trench 8F-2 also were analyzed; uranium-trend ages of 70 ± 10 and 80 ± 10 ka were determined on these two suites of samples. Estimates for the time of carbonate accumulation as rinds on pebbles in

the same alluvial fan deposit, using the conventional $^{230}\text{Th}/^{234}\text{U}$ method, were 41 ± 3 and 68 ± 4 ka.

INTRODUCTION

Uranium-series disequilibrium dating methods, described by Ku and others (1979), use conventional closed system $^{230}\text{Th}/^{234}\text{U}$ ratios for dating pedogenic carbonates which form rinds on alluvial gravel. These ages provide reasonable estimates of the minimum age of the alluvium. For conventional uranium-series dating (Ku, 1976), a closed system is assumed to exist throughout the history of a sample, which means that there has been no postdepositional migration of ^{238}U or of its daughter products (^{234}U and ^{230}Th). In contrast, open-system conditions impose no restrictions on migration. Results of other studies of uranium-series disequilibria indicate that uranium commonly exhibits an open-system behavior in many near-surface deposits (Ivanovich and Harmon, 1982). Because materials suitable for closed-system dating are commonly absent in Quaternary deposits in this area of the Great Basin, an open-system dating method is needed.

An open-system variation of uranium-series dating called uranium-trend dating has been tested extensively over the past decade. A preliminary model for uranium-trend dating was described by Rosholt (1980) with samples collected from a variety of Quaternary deposits including alluvium, eolian sediments, glacial deposits, and zeolitized volcanic ash. A revised model for uranium-trend systematics was described by Rosholt (1985). The empirical model requires time calibration based on analyses of deposits of known age; results of these calibrations are included in Rosholt and others (1985b). The uranium-trend ages of alluvium, colluvium, and eolian deposits at the Nevada Test Site area were reported by Rosholt and others (1985a).

For uranium-trend dating of sediments, the distribution of uranium-series members during and after sedimentation must have been controlled by open-system behavior. Sediments and soils are penetrated continuously or episodically with water that contains at least small amounts of transported or locally derived uranium. As this water-borne uranium decays, it produces a trail of radioactive daughter products that are readily adsorbed on solid matrix material. If the trail of the daughter products, ^{234}U and ^{230}Th , is distributed through the deposit in a consistent pattern, then uranium-trend dating is possible. The large number of

geochemical variables in an open system precludes the definition of a rigorous mathematical model for uranium migration. Instead, an empirical model is used to define the parameters that can reasonably explain the patterns of isotopic distribution.

This model requires independent time calibration with deposits of known age. None of the known-age deposits used for calibration occur in Nevada; however, results on other deposits in the Nevada Test Site region (Rosholt and others, 1985a) indicate that results obtained by the uranium-trend method are reasonable when compared to geomorphic and stratigraphic relations. In rare instances at NTS, ages can be compared by two methods (Swadley and others, 1984). At Crater Flat, a uranium-trend age of 270,000 years (270 ± 30 ka) was obtained for gravel deposits of unit Q2 of Swadley and Hoover (1983) that locally overlie and contain reworked cinders from a small volcano northwest of Lathrop Wells, Nev., which has yielded K-Ar ages ranging from 230 to 300 ka as determined by different laboratories (Vaniman and others, 1982).

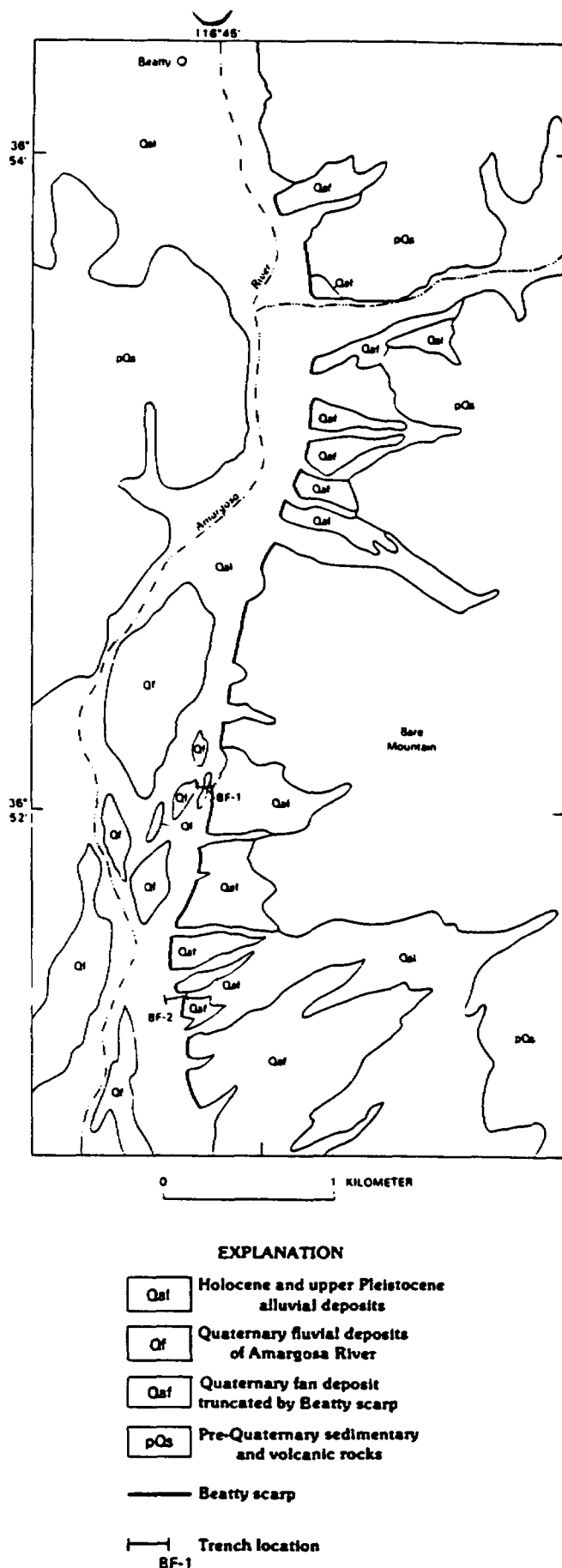
In an open-system environment, analyses of the abundances of ^{238}U , ^{234}U , ^{230}Th , and ^{232}Th in a single sample do not establish a meaningful time-related pattern of isotopic distribution. However, analyses of several samples, each of which has only slightly different physical properties and only slightly different chemical compositions within a unit, may provide a consistent pattern in the distribution of these isotopes (Rosholt, 1985). Analyses of five to eight samples per unit from several alluvial, colluvial, glacial, and eolian deposits has yielded time-related patterns (Rosholt and others, 1985a, b). These types of deposits range from clay-silt units to gravel units, most of which have isotopic distributions that appear to fit the model.

The purpose of this investigation is to apply the uranium-trend dating technique to the geologic study of surficial deposits along the Beatty scarp in southern Nevada (fig. 11.1). Conventional closed-system uranium-series dating was used to determine the time of carbonate accumulation as rinds on clasts in an alluvial fan truncated by the scarp. The surficial geology of the Beatty scarp site is described by Swadley and others (chapter 9).

Acknowledgments

We thank R.R. Shroba and D.R. Muhs for help collecting samples of the alluvial fan; D.R. Muhs for uranium-series ages and valuable help with interpretation of the age estimates and map illustrations; and N.C. Bostick and E.C. Spiker for the organic petrographic studies of the carbonaceous matter.

Figure 11.1. Generalized geology of Amargosa River area, Nevada, in vicinity of Beatty scarp (from Swadley and others, chapter 9).



SAMPLE COLLECTION, PREPARATION, AND CHEMICAL PROCEDURES

Several samples, about 1 kg each, were collected from a vertical section of each depositional unit. The number of samples required to establish a reliable linear trend in the data depends on the variation in ratios of uranium and thorium that define the trend line; our experience indicates that five to eight samples in a given unit are usually sufficient. It is preferable to collect samples from a channel cut through deposits exposed in a trench wall or a relatively fresh, well-exposed outcrop. Depositional units in the Nevada Test Site area commonly contain abundant pebbles and larger fragments, which are removed by sieving. The remaining less-than-2-mm-size fraction is pulverized to less than 0.2-mm size, homogenized, and retained for analysis. Chemical procedures used for separating uranium and thorium for alpha spectrometry measurements are those described by Rosholt (1985). Spikes of ^{236}U and ^{229}Th are used in the radioisotope-dilution technique to determine the concentrations of uranium and thorium (Rosholt, 1984). For defining uranium-trend slopes, each uranium separate is counted four different times in an alpha spectrometer, and each thorium separate is counted three different times. For conventional closed-system dating using $^{230}\text{Th}/^{234}\text{U}$ ratios, we sampled CaCO_3 rinds on the undersides of clasts found in the alluvial fan deposit above trench BF-2. Selective carbonate dissolution procedures followed Ku and Liang (1984) and chemical procedures followed Rosholt (1984, 1985). Ages were calculated using the isochron-plot method of Szabo and Sterr (1978).

SAMPLE SITES

Two trenches used in the evaluation of the origin and age of a scarp located near U.S. Highway 95 south of Beatty, are described in detail by Swadley and others (chapter 9); map-unit symbols used for these sites are discussed in there. Complete logs of these two trenches also are available (Swadley and others, 1986).

Trench BF-1 exposed interbedded gravel, sand, sandy silt, and clayey silt (unit Qf) that were deposited by the Amargosa River at the base of the scarp (fig. 11.1). Unit Qf is overlain by a thin deposit of silty alluvium (unit Q1c). Six sample suites, containing approximately eight samples each, were collected from the trench (fig. 11.2). Sample suites BF5 and BF6 are duplicate suites, collected 2.5 m apart, from the pebble-cobble gravel unit of Qf near the base of the trench.

An alluvial fan (units Q2a, Q2b, Q2c) truncated by the Beatty scarp near trench BF-2, 1.2 km south of trench BF-1, was sampled at two sites to estimate the age of this fan. Sample suite BT2F was collected from a 1.3-m-deep hole

excavated in the exposed side of the fan, approximately 50 m northwest of the trench. Sample suite 2BT2F was collected from a backhoe pit that penetrated the top of the same alluvial fan surface, approximately 55 m northwest of the trench. Stones found in the alluvial fan deposit, at 0.5 to 1 m depth, were sampled to estimate the time of carbonate accumulation in the fan; conventional uranium-series dating was used with analyses of CaCO_3 rinds on the undersides of the clast.

RESULTS

The analytical results for the eight sample suites are listed in table 11.1. Uranium and thorium contents are precise within ± 2 percent (1 sigma). Standard deviation for the $^{234}\text{U}/^{238}\text{U}$, $^{230}\text{Th}/^{238}\text{U}$, and $^{230}\text{Th}/^{232}\text{Th}$ ratios are 1.5, 2, and 1.5 percent, respectively, based on the precision of repeated counts of the chemical separates. The uranium-trend model parameters (Rosholt, 1985) and calculated ages of the eight suites are shown in table 11.2.

Uranium-trend plots of the results for alluvial fan sample suites (BT2F and 2BT2F) show acceptable ranges of isotopic ratios and good linearity (fig. 11.3), yielding estimated ages of 70 ± 10 ka and 80 ± 10 ka, respectively. Estimated times for the carbonate accumulation in the fan, 41 ± 3 ka and 68 ± 4 ka (table 11.3), are consistent with the approximate 75-ka uranium-trend ages for the fan deposit. For the two upper units from trench BF-1 (fig. 11.4) uranium-trend ages of 75 ± 10 ka and 155 ± 35 ka, respectively, were obtained. Results for two of the three lower fluvial units, (suites BF3 and BF4) indicate negative slopes (fig. 11.5) and uranium-trend ages of $+80 \pm 50$ ka and 530 ± 70 ka, respectively. Duplicate results for the deeper fluvial unit, (suites BF5 and BF6) are shown in figure 11.6; uranium-trend ages of 540 ± 100 ka and 460 ± 90 ka, respectively, were obtained. For the three lower fluvial units, the dating method does not provide sufficient resolution to distinguish differences in age. An average age and standard deviation of the values for the three units represented by suites BF3, BF4, and BF5-BF6 is 500 ± 60 ka.

Disseminated carbonized wood fragments (6 mm maximum size) occur in the fluvial clayey silt unit (suite BF3; fig. 11.2). A radiocarbon age of 10.0 ± 0.3 ka was obtained on this carbonaceous material (W-5673; Meyer Rubin, U.S.G.S., written commun., 1985). There is a great difference between the ^{14}C age (10 ka) and the uranium-trend age (480 ka) for this unit. After detailed petrographic study of the carbonaceous material, N.C. Bostick (written commun., 1985) determined that the carbon is not charcoal but coalified pure wood tissue. In a further study using ^{13}C nuclear magnetic resonance spectroscopy and element abundances (H, C, N, O), E.C. Spiker (written commun., 1986) found that the carbonized wood is similar to highly oxidized humic material although he could not rule out charcoal as a possible source of the material.

DISCUSSION

The uranium-trend ages indicate that fluvial sediments exposed in trench BF-1 were deposited over a time period extending from the middle into late Pleistocene. We consider these ages to be reliable because (1) plots of (^{234}U - ^{238}U / ^{238}U) versus (^{238}U - ^{230}Th)/ ^{238}U show good linearity and extension (Rosholt, 1985), (2) the ages have stratigraphic consistency, and (3) duplicate analyses of the same stratigraphic unit (suites BF5 and BF6) show concordance within experimental error. The uranium-trend ages suggest that all of the lowermost units were deposited about 500,000 yr ago, as dates are all concordant around this age within error limits. Suite BF2 yielded a significantly younger age of about 155 ka indicating a depositional hiatus between the units represented by suites BF3 and BF2 of about 345 ka. If the top of the fluvial silts (suites BF3) was exposed for about 345 ka before deposition of the upper fluvial gravels (suite BF2), then a well-developed paleosol should be present. The absence of a well-developed paleosol at the contact between these two units suggests a major period of erosion sometime between about 500 ka and about 160 ka. A similar interpretation can be made for the contact between the upper fluvial gravel (suite BF2) and the silty alluvium (suite BF1) at the surface; the dates suggest a depositional hiatus between about 155 ka and about 75 ka. Again, the absence of a well-developed paleosol at the contact between these two units also suggests a major period of erosion some time between about 155 ka and 75 ka.

The uranium-trend age estimate of the uppermost unit (Q1c, suite BF1) in trench BF-1 is difficult to evaluate geomorphically or pedologically, but some constraints are possible. There is only weak pedogenic carbonate development in unit Q1c, but a discontinuous, 2-cm-thick zone of CaCO_3 accumulation is found at depths of 40–50 cm. This material is 15–20 percent CaCO_3 , based on loss on ignition. If the carbonate is pedogenic, it indicates enough carbonate accumulation to suggest a pre-Holocene age for unit Q1c, based on rates of carbonate accumulation in alluvium in similar climates as summarized by Machette (1985). The surface there also has a weak stone pavement, with rock varnish found on the pavement clasts (fig. 11.2). Stone pavements can form in as short a time as a few years in arid regions (Sharon, 1962), but observations by many researchers indicate that rock varnish requires several thousand to as much as 10,000 years to form (Dorn and Oberlander, 1982). One can conclude from the combined carbonate and rock-varnish data that unit Q1c is probably older than earliest Holocene and perhaps considerably older.

The results from trench BF-1 suggest that a sequence of several alluvial deposits were laid down by the Amargosa River at the base of the Beatty scarp in the last 500,000 yr. The fan deposits actually cut by the Beatty scarp in the vicinity of trench BF-1 have not been dated because suitable sampling sites were not found. Presumably, they predate the oldest unit (~500 ka) exposed in trench BF-1 if the scarp is erosional and not tectonic. However, we have dated an alluvial fan truncated by the Beatty scarp approximately

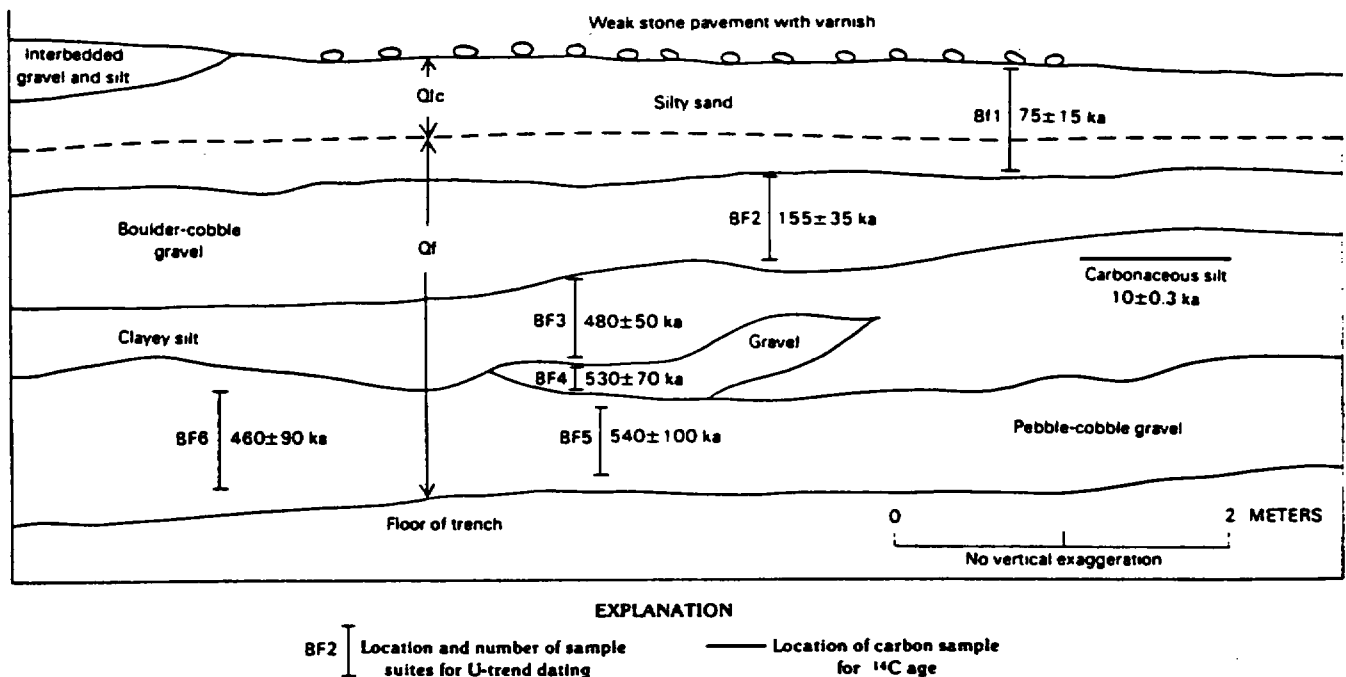


Figure 11.2. Diagram of sampled area on south face of trench BF-1 (fig. 11.1). Modified from trench log of Swadley and others (1986). Q1c, silty alluvium (Swadley and Hoover, 1983); Qf, fluvial sediments (Swadley and Hoover, 1983). Uranium-trend ages shown next to sample locations.

Table 11.1. Sample collection depth, element concentrations, and uranium-series activity ratios

Sample	Depth (cm)	Th (ppm)	U (ppm)	$^{234}\text{U}/^{238}\text{U}$	$^{230}\text{Th}/^{238}\text{U}$	$^{230}\text{Th}/^{232}\text{Th}$	$^{238}\text{U}/^{232}\text{Th}$
Sandy gravel of fan deposit (channel in outcrop)							
BT2F-1	36-47	7.74	1.18	1.149	1.138	0.538	0.473
BT2F-2	47-58	11.3	1.73	1.132	1.110	.523	.471
BT2F-3	58-69	11.2	1.76	1.157	1.133	.549	.485
BT2F-4	69-80	11.2	1.96	1.211	.986	.535	.542
BT2F-5	80-91	12.2	2.43	1.279	.830	.513	.617
BT2F-6	91-102	11.9	2.49	1.295	.837	.541	.647
BT2F-7	102-113	11.4	2.29	1.262	.904	.562	.622
BT2F-8	113-124	11.3	2.21	1.224	.959	.579	.604
Sandy gravel of fan deposit (channel in backhoe pit)							
2BT2F-2	28-38	10.7	1.53	1.112	1.241	0.547	0.441
2BT2F-3	38-48	11.2	1.51	1.101	1.187	.494	.416
2BT2F-4	48-58	11.3	1.71	1.166	1.087	.508	.468
2BT2F-5	58-68	10.7	2.16	1.312	.834	.523	.627
2BT2F-6	68-78	10.3	2.29	1.281	.849	.585	.690
2BT2F-7	78-88	10.9	2.20	1.260	.926	.577	.624
2BT2F-8	88-98	10.4	2.46	1.344	.834	.612	.734
Silty alluvium and fluvial sand, trench BF-1							
BF1-2	10-20	14.9	2.27	1.036	1.345	0.634	0.471
BF1-3	20-30	16.4	2.67	1.083	1.204	.607	.504
BF1-4	30-40	16.2	2.51	1.114	1.247	.596	.478
BF1-5	40-50	16.8	2.85	1.155	1.104	.583	.527
BF1-6	50-60	17.9	3.21	1.191	1.066	.598	.561
BF1-7	60-70	17.6	3.25	1.193	1.054	.607	.576
BF1-8	70-80	19.4	2.91	1.118	1.154	.536	.465
Fluvial gravel, trench BF-1							
BF2-1	35-93	16.5	2.99	1.127	1.040	0.581	0.558
BF2-2	93-101	17.9	3.33	1.158	1.008	.578	.574
BF2-3	101-109	17.8	3.27	1.151	.995	.564	.566
BF2-4	109-117	17.4	3.16	1.184	1.001	.569	.568
BF2-5	117-125	16.7	3.39	1.205	.953	.596	.626
BF2-6	125-133	17.6	3.33	1.142	1.011	.593	.587
BF2-7	133-141	17.7	3.30	1.120	1.033	.593	.574
BF2-8	141-149	18.4	3.06	1.099	1.145	.588	.513
Fluvial silt, trench BF-1							
BF3-1	150-157	19.7	3.36	1.323	1.327	0.699	0.527
BF3-2	157-164	19.4	3.35	1.247	1.170	.626	.535
BF3-3	164-171	17.1	2.94	1.227	1.139	.604	.531
BF3-4	171-178	14.8	2.50	1.234	1.153	.602	.522
BF3-5	178-185	17.6	2.95	1.290	1.219	.632	.519
BF3-6	185-192	20.2	3.35	1.449	1.366	.700	.512
BF3-7	192-199	15.4	2.70	1.312	1.282	.694	.542
BF3-8	199-206	18.1	2.93	1.293	1.332	.668	.501
Fluvial gravel, trench BF-1							
BF4-1	210-214	18.4	2.90	1.264	1.267	0.618	0.488
BF4-2	214-218	18.0	3.00	1.216	1.199	.616	.514
BF4-3	218-222	18.3	3.00	1.228	1.265	.641	.507
BF4-4	222-228	19.4	3.15	1.314	1.390	.697	.501
BF4-5	228-232	19.7	3.01	1.272	1.348	.637	.472
BF4-6	232-236	20.1	3.35	1.189	1.200	.616	.514

Table 11.1. Sample collection depths, element concentrations, and uranium-series activity ratios—Continued

Sample	Depth (cm)	Th (ppm)	U (ppm)	$^{234}\text{U}/^{238}\text{U}$	$^{230}\text{Th}/^{238}\text{U}$	$^{230}\text{Th}/^{232}\text{Th}$	$^{238}\text{U}/^{232}\text{Th}$
Fluvial gravel, trench BF-1							
BF5-1	244-250	18.8	2.92	1.163	1.204	0.577	0.479
BF5-2	250-256	17.7	2.71	1.188	1.168	.553	.473
BF5-3	256-262	19.3	2.85	1.133	1.072	.489	.457
BF5-4	262-268	20.0	2.90	1.227	1.219	.547	.449
BF5-5	268-274	18.7	2.74	1.187	1.149	.520	.452
BF5-6	274-280	19.7	2.73	1.182	1.136	.486	.428
BF5-7	280-286	20.2	2.88	1.145	1.100	.484	.440
BF5-8	286-292	19.2	2.65	1.225	1.272	.544	.427
BF6-1	222-232	16.7	2.60	1.180	1.175	.567	.482
BF6-2	232-242	16.4	3.00	1.265	1.144	.575	.502
BF6-3	242-252	18.4	3.07	1.131	1.070	.561	.525
BF6-4	252-262	18.1	3.06	1.187	1.131	.576	.509
BF6-5	262-272	18.5	2.84	1.142	1.079	.494	.458
BF6-6	272-282	19.1	3.03	1.137	1.098	.566	.516
BF6-7	282-292	18.2	2.91	1.133	1.094	.534	.488
BF6-8	292-302	18.4	3.06	1.238	1.106	.609	.551

Table 11.2. Uranium-trend model parameters and ages of depositional units in Beatty area
[F(0), uranium flux]

Sample suite	Description of deposit	U-trend slope	x intercept	Half period of F(0) (ka)	Age (ka)
Trench BF-2 area					
BT2F	Alluvial fan deposit adjacent to trench BF-2 (outcrop channel).	+0.487	-0.426	100	70±10
2BT2F	Alluvial fan deposit adjacent to trench BF-2 (backhoe pit channel).	+ .554	- .400	110	80±10
Trench BF-1					
BF1	Silty alluvium at surface-----	+ 0.538	- 0.404	100	75±154
BF2	Upper fluvial gravel-----	+ .588	- .275	200	155±35
BF3	Lower fluvial silt-----	- .753	+ .143	520	480±50
BF4	Lower fluvial gravel-----	- .570	+ .155	500	530±70
BF5	Lower fluvial gravel-----	- .490	+ .204	420	540±100
BF6	Lower fluvial gravel (same as BF5).	-2.071	- .026	680	460±90

1.2 km south of trench BF-1 (fig. 11.1); this fan is about 55 m northwest of trench BF-2. Samples taken from a natural exposure along the side of this fan yielded a uranium-trend age estimate of 70 ± 10 ka (table 11.2). In order to confirm this age, a backhoe pit was dug on a flat, stable part of the

fan surface, and samples collected there gave a concordant uranium-trend age estimate of 80 ± 10 ka (table 11.2). In both cases, the uranium-trend plots are highly linear (correlation coefficients are both 0.98, significant at the 99.9 percent confidence level).

As a further test of the uranium-trend age estimates, carbonate rinds from fan clasts were collected in the pit from depths of about 0.5–1.0 m; the rinds are 1–3 mm thick. Two samples were analyzed for conventional closed-system

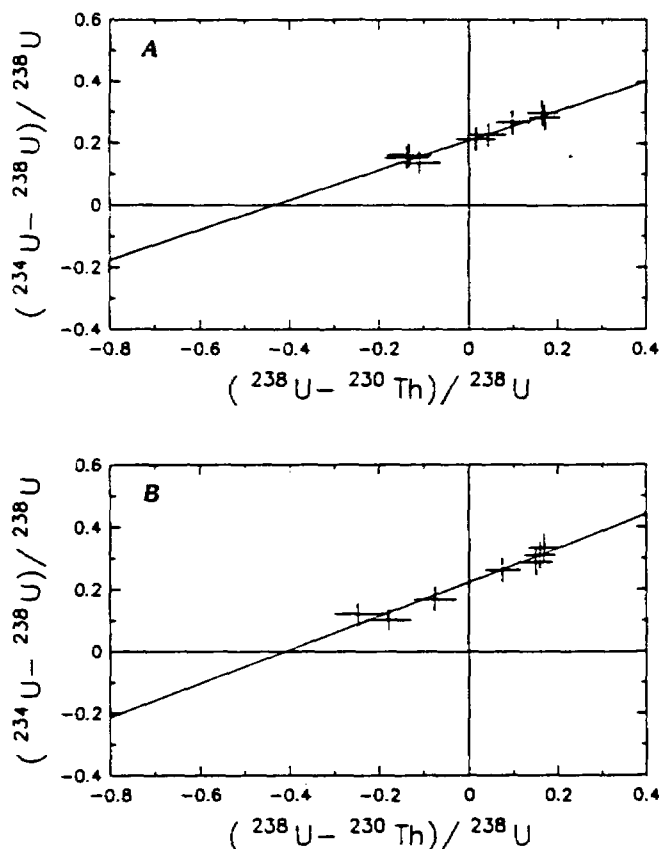


Figure 11.3. Uranium-trend plot of fan alluvium adjacent to trench BF-2 (fig. 11.1). A, Suite BT2F. B, Suite 2BT2F. The x-intercept is where regression line intersects zero line for $(^{234}\text{U} - ^{238}\text{U})/^{238}\text{U}$.

$^{230}\text{Th}/^{234}\text{U}$ dating that yielded age estimates of 41 ± 3 ka and 68 ± 4 ka (table 11.3). These age estimates support the uranium-trend age estimates, because the uranium-trend ages theoretically date the time of deposition of the alluvial fan materials whereas the uranium-series dates should be time integrated age estimates of the period of carbonate accumulation. Because carbonate accumulation had to occur after the fan deposits were stabilized, uranium-series age estimates for the carbonate should be no older than uranium-trend dates of the fan deposits themselves.

Finally, all radiometric determinations on these fan deposits are supported by pedologic and rock-varnish data. The surface of the fan has a well-developed stone pavement, and clasts in the pavement have been strongly varnished. The soil developed in the fan deposits has Stage II carbonate morphology following the scheme of Gile and others (1966). Soils in similar climates with a Stage II carbonate morphology have been estimated to be roughly 60,000 to 120,000 yr old, based on previous uranium-series dates (Ku and others, 1979) and observations summarized by Machette (1985).

The significance of the age estimates of the fan deposits near trench BF-2 is that they provide a maximum age for the Beatty scarp, because they are exposed in the scarp. The results of our studies here are inconsistent with the results from trench BF-1, which suggest that the Beatty scarp is older than ~ 500 ka. Several interpretations of this apparent inconsistency are possible: (1) the alluvial deposits exposed in trench BF-1 may be downfaulted sediments, rather than deposits set in by fluvial processes against a preexisting erosional scarp, in which case the Beatty scarp is of tectonic origin (but see discussion in Swadley and others, chapter 9); (2) the Beatty scarp may have different ages at different localities; or (3) some of the uranium-trend age estimates in the lower units exposed in trench BF-1 may be too old, despite the fact that they meet all criteria for reliable age estimates.

Table 11.3. Concentrations, isotopic activity ratios, and uranium-series age estimates for carbonate pebble rinds in alluvial fan deposits near Beatty trench 2

Sample	CaCO ₃ (pct)	Th (ppm)	U (ppm)	$^{234}\text{U}/^{238}\text{U}$	$^{230}\text{Th}/^{232}\text{Th}$	$^{230}\text{Th}/^{234}\text{U}$	$^{234}\text{U}/^{238}\text{U}$	$^{230}\text{Th}/^{234}\text{U}$	Age estimate (ka)
2BT2F-A	91								
leachate-----		1.7	1.18	1.71 ± 0.03	1.41 ± 0.02	0.39 ± 0.01	1.91 ± 0.06	0.32 ± 0.01	41 ± 3
residue-----		8.5	1.37	$1.07 \pm .08$	$.42 \pm .01$	$.79 \pm .01$	----	----	----
2BT2F-B	78								
leachate-----		0.70	1.82	$1.72 \pm .02$	$6.7 \pm .1$	$.49 \pm .01$	$1.76 \pm .04$	$.48 \pm .02$	68 ± 4
residue-----		5.7	2.60	$1.55 \pm .02$	$1.13 \pm .02$	$.52 \pm .01$	----	----	----

*Corrected for detrital ^{230}Th and U contamination using the isochron-plot method of Szabo and Sterr (1978). Errors reported are based on multiple alpha counts in different detectors ($\pm 1\sigma$).

A serious inconsistency arises from comparison of the uranium-trend age of 480 ka for suite BF3 and a ^{14}C date on carbonaceous material collected from this same unit. The carbonaceous material yielded a ^{14}C date of 10 ka. The results of the petrographic study that indicate the carbonaceous material is coalified wood tissue rather than charcoal suggests that the carbon may be decomposed remnants of abundant root growth that penetrated the clayey silt horizon about 10 ka. We were not able to determine the exact source of the carbon using ^{13}C nuclear magnetic resonance spectroscopy.

CONCLUSIONS

The following conclusions can be made, based on uranium-trend ages on fluvial deposits from trench BF-1:

(1) deposition of silt, sand, and gravel took place at about 500, 155 and 75 ka; and (2) erosion took place between 500 and 155 ka, and again between 155 and 75 ka as indicated both by the differences in age and by the absence of well-developed paleosols between depositional units.

From uranium-trend and uranium-series ages and soil development on fans near trench BF-2, we conclude that the Beatty scarp at that locality is no older than about 80 ka. This conclusion is not consistent with the chronology and stratigraphic relations at trench BF-1, which suggests that (1) the Beatty scarp may be of tectonic origin, (2) the Beatty scarp may have different ages at different localities, or (3) some of our age estimates in the lower units of trench BF-1 may be too old. No unambiguous interpretation will be possible without further age control and more detailed examination of the field relations.

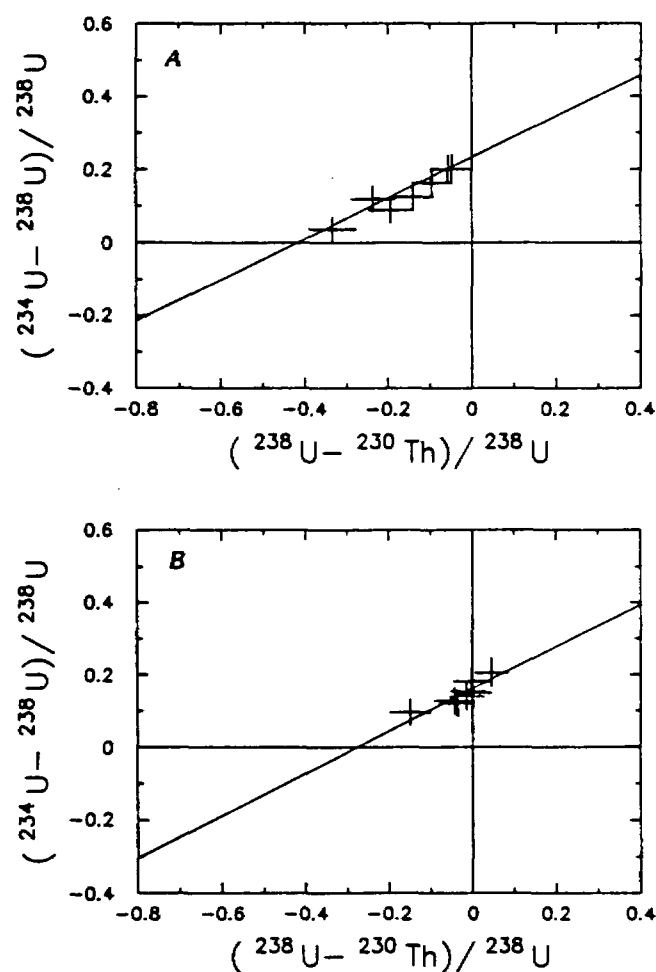


Figure 11.4. Uranium-trend plots of alluvium and fluvial deposit in trench BF-1 (fig. 11.1). A, Suite BF1. B, Suite BF2. The x-intercept is where regression line intersects zero line for $(^{234}\text{U} - ^{238}\text{U})/^{238}\text{U}$.

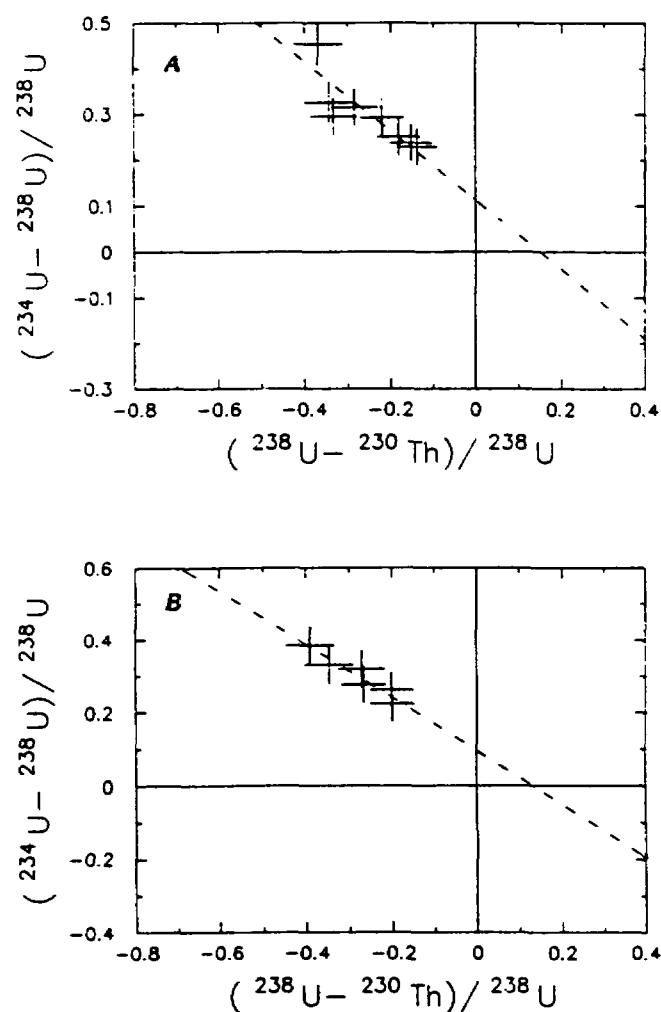


Figure 11.5. Uranium-trend plots of fluvial deposits in trench BF-1 (fig. 11.1). A, Suite BF3. B, Suite BF4. The x-intercept is where regression line intersects zero line for $(^{234}\text{U} - ^{238}\text{U})/^{238}\text{U}$.

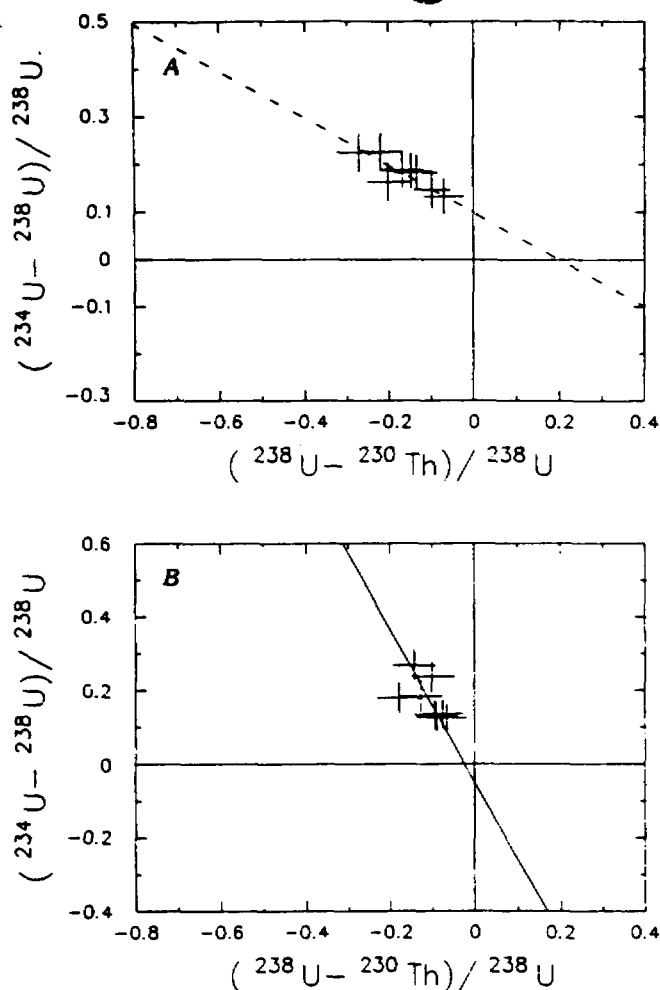


Figure 11.6. Uranium-trend plots of fluvial deposits in trench BF-1 (fig. 11.1). A, Suite BF5. B, Suite BF6. The x-intercept is where regression line intersects zero line for $(^{234}\text{U} - ^{238}\text{U})/^{238}\text{U}$.

REFERENCES CITED

- Dorn, R.I., and Oberlander, T.M., 1982, Rock varnish: Progress in Physical Geography, v. 6, p. 317-367.
- Gile, L.H., Peterson, F.F., and Grossman, R.B., 1966, Morphological and genetic sequences of carbonate accumulation in desert soils: Soil Science, v. 101, p. 347-360.
- Ivanovich, M., and Harmon, R.S., 1982, Uranium series disequilibrium: applications to environmental problems: Oxford, Clarendon Press, 571 p.
- Ku, T.L., 1976, The uranium-series methods of age determination: Annual Review, Earth and Planetary Science Letters, v. 4, p. 347-379.
- Ku, T.L., Bull, W.B., Freeman, S.T., and Knauss, K.G., 1979, $\text{Th}^{230}\text{-U}^{234}$ dating of pedogenic carbonates in gravelly desert soils of Vidal Valley, southeastern California: Geological Society of America Bulletin, v. 90, p. 1063-1073.
- Ku, T.L., and Liang, Z.C., 1984, The dating of impure carbonates with decay series isotopes: Nuclear Instruments and Methods in Physics Research, v. 223, p. 563-571.
- Machette, M.N., 1985, Calcic soils and calcretes of the southwestern United States, in Weide, D. L., ed., Soils and Quaternary geology of the southwestern United States: Geological Society of America Special Paper 203, p. 1-21.
- Rosholt, J.N., 1980, Uranium-trend dating of Quaternary sediments: U.S. Geological Survey Open-File Report 80-1087, 65 p.
- , 1984, Radioisotope dilution analyses of geological samples using ^{236}U and ^{229}Th : Nuclear Instruments and Methods in Physics Research, v. 223, p. 572-576.
- , 1985, Uranium-trend systematics for dating Quaternary sediments: U.S. Geological Survey Open-File Report 85-298, 34 p.
- Rosholt, J.N., Bush, C.A., Carr, W.J., Hoover, D.L., Swadley, W.C., and Dooley, J.R., Jr., 1985a, Uranium-trend dating of Quaternary deposits in the Nevada Test Site area, Nevada and California: U.S. Geological Survey Open-File Report 85-540, 72 p.
- Rosholt, J.N., Bush, C.A., Shroba, R.R., Pierce, K.L., and Richmond, G.M., 1985b, Uranium-trend dating and calibrations for Quaternary sediments: U.S. Geological Survey Open-File Report 85-299, 48 p.
- Sharon, D., 1962, On the nature of hamadas in Israel: Zeitschrift für Geomorphologie, v. 6, p. 129-147.
- Swadley, W.C. and Hoover, D.L., 1983, Geology of faults exposed in trenches in Crater Flat, Nye County, Nevada: U.S. Geological Survey Open-File Report 83-608, 15 p.
- Swadley, W.C., Hoover, D.L., and Rosholt, J.N., 1984, Preliminary report on late Cenozoic faulting and stratigraphy in the vicinity of Yucca Mountain, Nye County, Nevada: U.S. Geological Survey Open-File Report 84-788, 42 p.
- Swadley, W.C., Huckins, H.E., and Taylor, E.M., 1986, Logs of the trenches across the Beatty Scarp, Nye County, Nevada: U.S. Geological Survey Miscellaneous Field Studies Map MF-1897.
- Szabo, B.J., and Sterr, H., 1978, Dating caliches from southern Nevada by $^{230}\text{Th}/^{232}\text{Th}$ versus $^{234}\text{U}/^{232}\text{Th}$ and $^{234}\text{U}/^{232}\text{Th}$ versus $^{238}\text{U}/^{232}\text{Th}$ isochron-plot method, in Zartman, R. E., ed., Short papers of the 4th International Conference on Geochronology, Cosmochronology and Isotope Geology: U.S. Geological Survey Open-File Report 78-701, p. 416-418.
- Vaniman, D.T., Crowe, B.M., and Gladney, E.S., 1982, Petrology and geochemistry of hawaiite lavas from Crater Flat, Nevada: Contributions to Mineralogy and Petrology, v. 80, p. 341-357.

1415-

USGS-OFR-85-224

USGS-OFR-85-224

UNITED STATES
DEPARTMENT OF THE INTERIOR
GEOLOGICAL SURVEY

URANIUM, THORIUM ISOTOPIC ANALYSES AND URANIUM-SERIES AGES OF CALCITE AND
OPAL, AND STABLE ISOTOPIC COMPOSITIONS OF CALCITE FROM DRILL CORES
UE25a#1, USW G-2 AND USW G-3/GU-3, YUCCA MOUNTAIN, NEVADA

By

B. J. Szabo¹ and T. K. Kyser²

SAI
T&MSS
LIBRARY

¹ U.S. Geological Survey, Denver, CO

² University of Saskatchewan, CANADA

CONTENTS

	Page
Abstract.....	1
Introduction.....	1
Experimental procedures.....	2
Result and discussion.....	5
Summary.....	21
Acknowledgements.....	22
References.....	23

ILLUSTRATIONS

	Page
Figure 1. Location of Yucca Mountain, the Nevada Test Site and localities of drill holes.....	3
2. Histogram of uranium concentrations in calcite, uraniferous opal and acid insoluble residues.....	10
3. Calculated uranium-series dates ($\times 10^3$ years) of fracture and cavity filling calcite and opal in drill holes area plotted against corresponding depths in meters. Bars indicate experimental errors.....	13
4-A. Photomicrograph (A) and corresponding fission track image.....	14
4-B. (B) of uranium distribution in calcite and opal at 348.8 m depth in drill core USW G-2. Scale is 3x5 mm using cross-polar light. Uranium appears as dark shading in the fission track image in B; the lighter, banded regions show uranium redistribution due to partial crystallization of the amorphous secondary opal and the white area corresponds to low uranium calcite.....	15
5. $\delta^{18}O$ values of calcite from drill holes and surface travertines are plotted against depth of sample.....	17
6. Relationship between the $\delta^{13}C$ value and depth of calcite from the Yucca Mountain area.....	18
7. $\delta^{18}O$ versus the $\delta^{13}C$ values of calcite from Yucca Mountain. Lines and temperatures represent the calculated isotopic composition of calcite in equilibrium with meteoric water having a $\delta^{18}O$ value of -9 and $\delta^{13}C$ values of either -11.5 (lower line, hole USW G-2) or -8 (upper line, hole USW G-3). Fractionation factors for oxygen are those suggested by O'Neil and others (1969) and for carbon are those derived by Friedman 1970). The depth of some of the samples in meters are indicated in parentheses.....	21

UNITED STATES
DEPARTMENT OF THE INTERIOR
GEOLOGICAL SURVEY

URANIUM, THORIUM ISOTOPIC ANALYSES AND URANIUM-SERIES AGES OF CALCITE AND
OPAL, AND STABLE ISOTOPIC COMPOSITIONS OF CALCITE FROM DRILL CORES
JE25a#1, USW G-2 AND USW G-3/JS-3, YUCCA MOUNTAIN, NEVADA

By

B. J. Szabo and T. K. Kyser

ABSTRACT

Fracture and cavity filling calcite and opal in the unsaturated zone of three drill cores at Yucca Mountain were analyzed for uranium and stable isotope contents, and were dated by the uranium-series method. Stable isotope data indicate that the water from which the calcite precipitated was meteoric in origin. The decrease in ^{18}O and increase in ^{13}C with depth are interpreted as being due to the increase in temperature in drill holes corresponding to an estimated maximum geothermal gradient of 43° per km. Of the eighteen calcite and opal deposits dated, four of the calcite and all four of the opal deposits yield dates older than 400,000 years and ten of the remaining calcite deposits yield dates between 26,000 and 310,000 years. The stable isotope and uranium data together with the finite uranium-series dates of precipitation suggest complex history of fluid movements, rock and water interactions, and episodes of fracture filling during the last 310,000 years.

INTRODUCTION

Tertiary ash-flow tuffs of Yucca Mountain in southwestern Nevada are being considered as possible hosts for a repository for high-level radioactive waste. Initial examination of exploratory cores revealed that fractures and

cavities are commonly coated and in some cases are completely filled with secondary calcite and opal together with occasional trace amounts of manganese and iron oxides. Apparently these secondary minerals were precipitated from percolating groundwater that became saturated with calcite and silica by leaching wall rocks and fault gouge materials. The purpose of this study is to use the stable isotopic composition of the calcite to determine the origin of the fluids passing through fractures, and to attempt to determine the ages of calcite and opal samples by the uranium-series dating method.

EXPERIMENTAL PROCEDURES

Samples of calcite and opal were collected from the unsaturated zones of three drill holes at Yucca Mountain, Nevada: UE25a#1, USW G-2 and USW G-3/GU-3 (fig. 1). Geologic descriptions and results of geophysical measurements of the drill holes are reported by Hagstrum and others, 1980; Maldonado and Koether, 1983; and Scott and Castellanos, 1984. The thickness of the calcite and opal deposits sampled from these cores vary between about 1 mm and 1 cm. The calcite and opal coating was chipped or scrapped from the bed rock surfaces and fragments showing little or no wall rock contamination were hand-picked for subsequent analyses. Samples containing opal were checked for fluorescence under ultraviolet light. Opals exhibiting yellow-green light emission under ultraviolet stimulus are referred to as uraniferous opal in contrast to other silica which produced no noticeable fluorescence. Samples which were predominantly calcite were separated from occasional uraniferous opal fragments by hand-picking under ultraviolet light illumination. Samples that contained mixtures of calcite and uraniferous opal were collected together and were subjected to acid treatment for separation of calcite from opal, as discussed later.

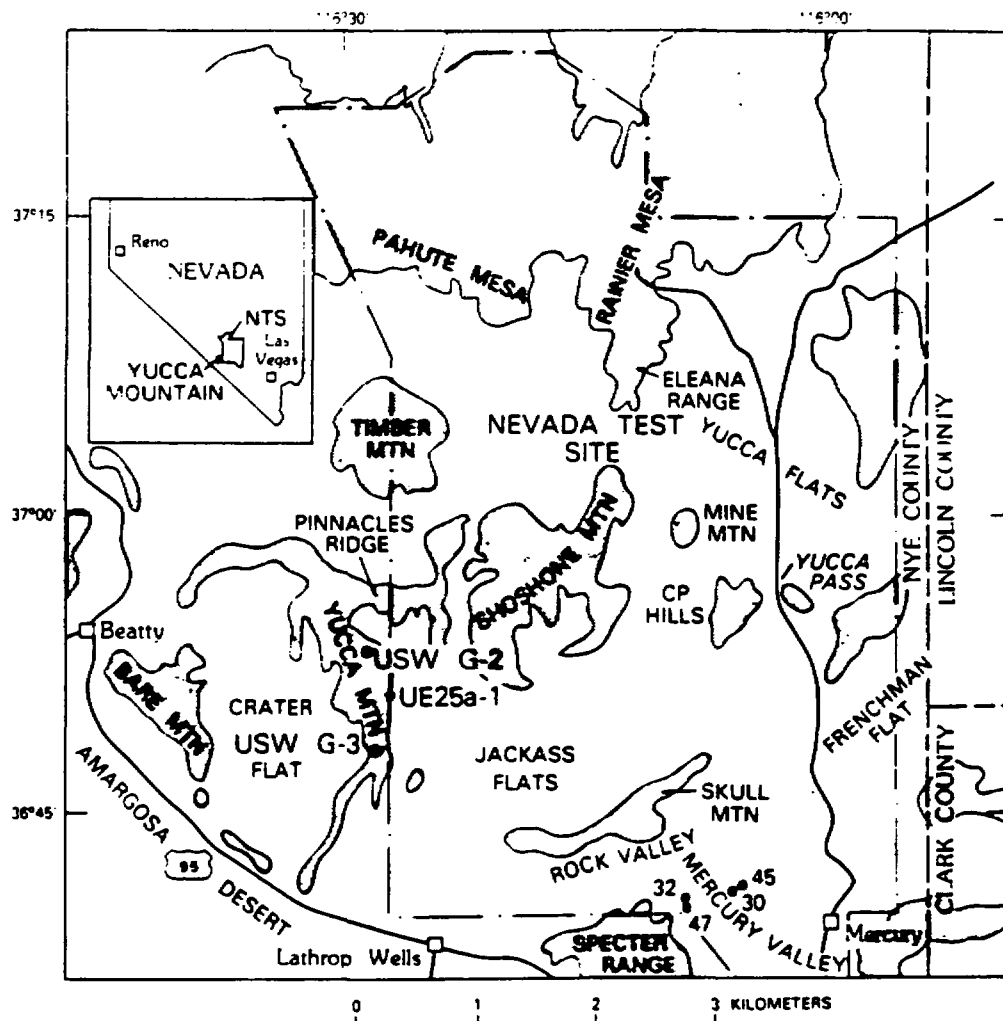


Figure 1. Location of Yucca Mountain, the Nevada Test Site and localities of drill holes.

Portions of calcite from the veins were dissolved in 100 percent phosphoric acid and the released CO_2 gas was analyzed in an isotope ratio mass spectrometer for carbon and oxygen isotopic compositions. The values are reported in the familiar delta notation as the $^{13}\text{C}/^{12}\text{C}$ or $^{18}\text{O}/^{16}\text{O}$ ratio in the sample relative to the ratios in a standard such that $\delta^{13}\text{C}$ or $\delta^{18}\text{O} = (R_{\text{sample}}/R_{\text{standard}} - 1) \times 1000$ where $R = ^{13}\text{C}/^{12}\text{C}$ or $^{18}\text{O}/^{16}\text{O}$. Standard mean ocean water (SMOW) is the standard for oxygen and a belemnite from the Pee Dee Formation in North Carolina is the standard for carbon. Using these techniques, we obtained a $\delta^{18}\text{O}$ value of +7.20 and a $\delta^{13}\text{C}$ value of -5.00 for NBS-18 carbonatite, in agreement with other laboratories.

Pure calcite samples selected for uranium-series analysis were ground to a fine powder and heated for a period of about 8 hours at 900°C to convert CaCO_3 to CaO . The samples were then dissolved in 8 F (formal) solution of HCl and spiked with ^{235}U , ^{229}Th , and ^{223}Th standard solution. Uranium and thorium isotopes were isolated and purified using an anion-exchange procedure described by Szabo and others (1981). Isolated and purified uranium was electroplated onto a platinum disc. Purified thorium was extracted in a small amount of 0.4 F thenoyltrifluoroacetone (TTA) in benzene and evaporated onto a stainless steel disc. Both discs were counted in an alpha spectrometer.

Mixtures of calcite and opal, or calcite and wall-rock were heated for a period of about 8 hours at 900°C converting calcite to CaO , then were separated by dissolving CaO in dilute nitric acid solutions (0.25 to 1.0 F HNO_3 , depending on sample size). The weighed sample was added to continuously stirred solution of nitric acid in small portions to prevent the slurry turning basic. The final acidity was adjusted to about pH 2, and the soluble and insoluble fractions were separated by centrifuging.

The soluble carbonate fraction was spiked with ^{235}U , ^{228}Th , and ^{229}Th and evaporated to a smaller volume. Uranium and thorium were coprecipitated with hydroxides of iron and aluminum by addition of concentrated NH_4OH , then the precipitate was dissolved in 8 F HNO_3 solution. The acid-insoluble fraction (opal and/or wall-rock particles) was spiked with ^{235}U , ^{228}Th , and ^{229}Th and dissolved by repeated refluxing with concentrated HF-HClO_4 mixtures. After taken to dryness, the residue was dissolved in 8 F HCl solution. For both fractions, the dissolved uranium and thorium were separated and purified by anion-exchange, and the discs were prepared and measured as described above.

RESULTS AND DISCUSSION

Uranium-series and stable isotopic data for fracture-filling calcite and opal samples from drill holes UE25a#1, USW G-2 and USW G-3/GU-3 at Yucca Mountain are shown in tables 1, 2, and 3. Errors reported for the uranium and thorium measurements are 1 σ propagated errors. All δ values are accurate to ± 0.15 (2 σ).

The uranium concentrations of the calcite, acid-insoluble residues, and uraniferous opal samples vary from about 0.01 to 58 ppm (fig. 2). The uranium concentrations of the carbonate samples range between about 0.01 and 5.0 ppm with the exception of sample 348.8-B which has an unusually high uranium content of 33.3 ppm (table 2). The uranium contents in the residue fractions consisting mainly of secondary silica and bedrock minerals vary between about 0.7 and 7 ppm and the uranium concentrations of the uraniferous opal samples range between about 15 and 58 ppm.

The calculated uranium-series dates of the fracture filling calcite and opal samples from drill holes at the Yucca Mountain area are listed in table 4. The dates of calcite free of acid-insoluble residue and of opal samples

Table 1. Analytical data of fracture filling calcite and acid-insoluble wall rock material from drill hole UE25a#1 at the Yucca Mountain area

Sample depth (m)	Material	Uranium (ppm)	$^{234}\text{U}/^{238}\text{U}$	$^{230}\text{Th}/^{232}\text{Th}$ (activity ratio)	$^{230}\text{Th}/^{234}\text{U}$	$\delta^{13}\text{C}$ (‰)	$\delta^{18}\text{O}$ (‰)
34	Calcite	0.767 ± 0.015	1.17 ± 0.02	2.37 ± 0.07	1.02 ± 0.04	-4.52	+20.00
87	Fault gouge	5.18 ± 0.10	1.09 ± 0.02	0.989 ± 0.030	1.06 ± 0.04	n.a.	n.a.
283	Calcite	5.03 ± 0.10	1.47 ± 0.02	22.2 ± 0.7	1.04 ± 0.04	-6.33	+17.50
611	Calcite	3.43 ± 0.07	1.29 ± 0.02	72 ± 3	1.19 ± 0.05	-5.41	+15.60

n.a. not applicable.

Table 2. Analytical data of fracture filling calcite, uraniferous opal and acid insoluble residue fractions from drill hole USW G-2 at the Yucca Mountain area

Sample depth (m)	Fraction	Percent carbonate	Uranium (ppm)	$^{234}\text{U}/^{238}\text{U}$	$^{230}\text{Th}/^{232}\text{Th}$	$^{230}\text{Th}/^{234}\text{U}$	$\delta^{13}\text{C}$	$\delta^{18}\text{O}$
				(activity ratio)			(‰)	(‰)
280	Calcite	>99	0.500 ± 0.010	1.032 ± 0.015	12.0 ± 2.4	1.023 ± 0.041	-8.35	+19.21
302	Calcite	n.d.	n.d.	n.d.	n.d.	n.d.	-7.90	+19.31
346.7	Calcite	64	0.405 ± 0.008	1.167 ± 0.018	4.29 ± 0.21	0.915 ± 0.037	-7.43	+18.22
	Residue	0	6.85 ± 0.14	1.135 ± 0.017	2.43 ± 0.10	0.965 ± 0.049	n.a.	n.a.
346.8	Calcite	n.d.	n.d.	n.d.	n.d.	n.d.	-7.37	+18.30
348.7	Calcite	>99	0.073 ± 0.006	1.02 ± 0.03	4.6 ± 0.5	0.73 ± 0.06	-7.47	+18.19
348.8-A	Calcite	97	0.136 ± 0.004	0.937 ± 0.028	10.7 ± 1.6	1.010 ± 0.040	-6.93	+18.13
348.8-B	Calcite	63	33.3 ± 0.7	1.026 ± 0.015	94 ± 15	0.093 ± 0.037	n.d.	n.d.
	U Opal	0	57.8 ± 1.2	1.031 ± 0.015	232 ± 34	1.027 ± 0.031	n.d.	n.d.
359-A	Calcite	61	1.21 ± 0.06	1.020 ± 0.015	261 ± 80	0.795 ± 0.032	-6.82	+17.98
359-B	Calcite	75	0.644 ± 0.013	0.965 ± 0.014	36 ± 11	0.811 ± 0.032	n.d.	n.d.
	U Opal	0	27.0 ± 0.5	1.068 ± 0.016	234 ± 70	1.04 ± 0.04	n.d.	n.d.
361	Calcite	n.d.	n.d.	n.d.	n.d.	n.d.	-6.56	+17.77

n.d. not determined

n.a. not applicable

Table 3. Analytical data of fracture filling calcite, uraniferous opal and acid insoluble residues from drill hole USW G-3/GU-3 at the Yucca Mountain area

Sample depth (m)	Fraction	Percent carbonate	Uranium (ppm)	$^{234}\text{U}/^{238}\text{U}$ (activity ratio)	$^{230}\text{Th}/^{232}\text{Th}$ (activity ratio)	$^{230}\text{Th}/^{234}\text{U}$ (activity ratio)	$\delta^{13}\text{C}$ (‰)	$\delta^{18}\text{O}$ (‰)
63	Calcite	95	0.553 ± 0.011	2.26 ± 0.03	35 ± 4	1.00 ± 0.03	-7.06	+20.23
	Residue	n.a.	0.66 ± 0.04	1.37 ± 0.10	7.6 ± 1.5	1.94 ± 0.19	n.a.	n.a.
131	Calcite	52	3.02 ± 0.06	1.43 ± 0.02	84 ± 40	0.216 ± 0.009	-5.11	+20.16
	U Opal	n.a.	35.0 ± 0.7	1.13 ± 0.02	473 ± 190	1.15 ± 0.05	n.d.	n.d.
147	Calcite	n.d.	n.d.	n.d.	n.d.	n.d.	-5.58	+20.04
159	Calcite	n.d.	n.d.	n.d.	n.d.	n.d.	-5.44	+20.28
318	Calcite	95	0.0836 ± 0.0017	0.991 ± 0.020	2.58 ± 0.13	1.10 ± 0.06	-5.10	+19.11
	Residue	n.a.	1.88 ± 0.11	0.73 ± 0.07	4.89 ± 0.73	1.27 ± 0.13	n.a.	n.a.
331	Calcite	87	0.36 ± 0.01	1.06 ± 0.04	10 ± 5	0.24 ± 0.02	-4.54	+18.73
	U Opal	n.a.	14.9 ± 0.4	1.05 ± 0.03	153 ± 61	1.13 ± 0.06	n.d.	n.d.

n.a. not applicable

n.d. not determined

Table 4. Calculated uranium-series ages of fracture filling calcite and opal from drill holes at the Yucca Mountain area, Nevada

Drill hole	Depth (m)	Uranium (ppm)	Calculated age ($\times 10^3$ years)
Calcite			
UE25a#1	34	0.77	310_{-50}^{+80} (a)
GU-3	63	0.56	227 ± 20
GU-3	131	3.0	26 ± 2
USW-G-2	280	0.50	>400
UE25a#1	293	5.0	310_{-45}^{+70}
GU-3	318	0.084	>400
GU-3	331	0.36	30 ± 4
USW-G-2	346.7	0.40	190 ± 20 (b)
USW-G-2	348.7	0.073	142 ± 30
USW-G-2	348.8-A	0.14	>400
USW-G-2	348.8-B	33	280 ± 70
USW-G-2	359-A	1.2	170 ± 18
USW-G-2	359-B	0.64	185 ± 18
UE25a#1	611	3.4	>400
Uraniferous Opal			
GU-3	131	35	>400
GU-3	331	15	>400
USW-G-2	348.8-B	58	>400
USW-G-2	359-B	27	>400

a. Isochron-plot corrected using analytical data of fault gouge.

b. Isochron-plot corrected using analytical data of both acid-soluble carbonate and acid-insoluble residue.

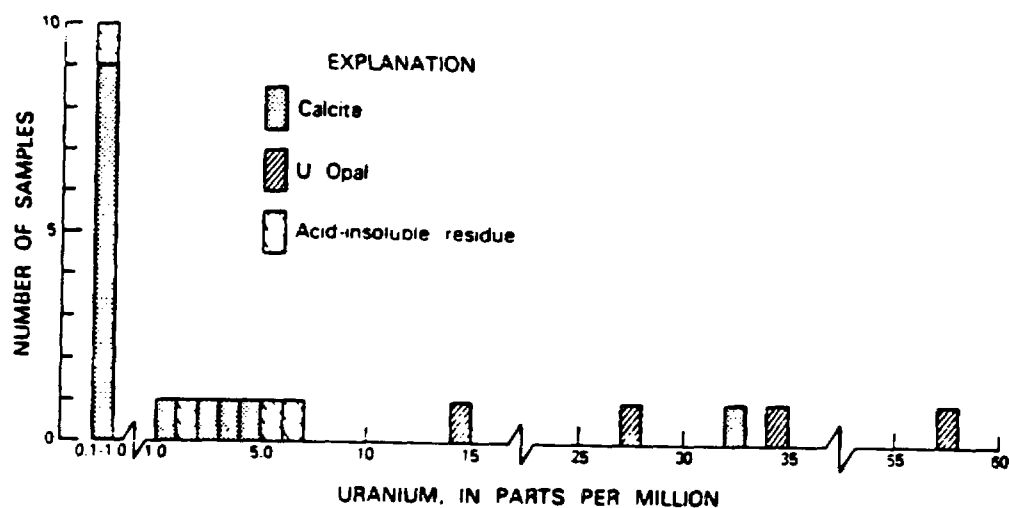


Figure 2. Histogram of uranium concentrations in calcite, uraniferous opal and acid insoluble residues.

Table 4. Calculated uranium-series ages of fracture filling calcite and opal from drill holes at the Yucca Mountain area, Nevada

Drill hole	Depth (m)	Uranium (ppm)	Calculated age ($\times 10^3$ years)
Calcite			
UE25a#1	34		310^{+80}_{-50} (a)
GU-3	63	0.56	227 ± 20
GU-3	131	3.0	26 ± 2
USW-G2	280	0.50	>400
UE25a#1	283	5.0	310^{+70}_{-45}
GU-3	318	0.084	>400
GU-3	331	0.36	30 ± 4
USW-G-2	346.7	0.40	190 ± 20 (b)
USW-G-2	348.7	0.073	142 ± 30
USW-G-2	348.8-A	0.14	>400
USW-G-2	348.8-B	33	280 ± 70
USW-G-2	359-A	1.2	170 ± 18
USW-G-2	359-B	0.64	185 ± 18
UE25a#1	611	3.4	>400
Uraniferous Opal			
GU-3	131	35	>400
GU-3	331	15	>400
USW-G-2	348.8-B	58	>400
USW-G-2	359-B	27	>400

a. Isochron-plot corrected using analytical data of fault gouge.

b. Isochron-plot corrected using analytical data of both acid-soluble carbonate and acid-insoluble residue.

are calculated from their measured $^{230}\text{Th}/^{234}\text{U}$ activity ratios using standard radioactive growth and decay equations assuming that the authigenic calcite and opal had remained ideal closed systems with respect to the isotopes of uranium and thorium since their formation. In contrast, the dates for impure calcite samples were calculated using the results for the acid-soluble and acid-insoluble fractions in a pseudo-isochron-plot method described by Szabo and others (1981), and Szabo and Rosholt (1982).

Uranium-series dates of fracture-filling calcite samples range from 26,000 to >400,000 years and uranium-series dates of uraniferous opal samples are all older than 400,000 years. The dates are plotted against their corresponding depths in fig. 3. Depth intervals lacking dated samples, however, may not be real because we arbitrarily selected the thicker deposits best suited for dating. Two calcite samples yield an average date of 28,000 years, four calcite deposits yield an average date of about 170,000 years and four calcite deposits have an average date of about 280,000 years. In addition, four calcite and four uraniferous opal deposits are yielding minimum dates of precipitation of greater than 400,000 years. The distribution of the finite calcite dates suggests fluid movement and fracture and cavity filling in these drill holes between 26,000 and 310,000 years.

The distribution of uranium in uraniferous opal at 348.8 m depth in drill hole USW G-2 was determined by fission-track mapping. A photomicrograph of the uraniferous infilling in the host calcite is shown in fig. 4-A and the corresponding fission-track image is displayed in fig. 4-B. The dark areas in fig. 4-B correspond to localities of uraniferous opal, the lighter-colored area are the partially crystallized opal of lower uranium content, and the lightest area is the host calcite of the lowest uranium content. Bulk uranium analysis of the separated calcite (0.136 ppm U-sample 348.8-A, table 2) and of

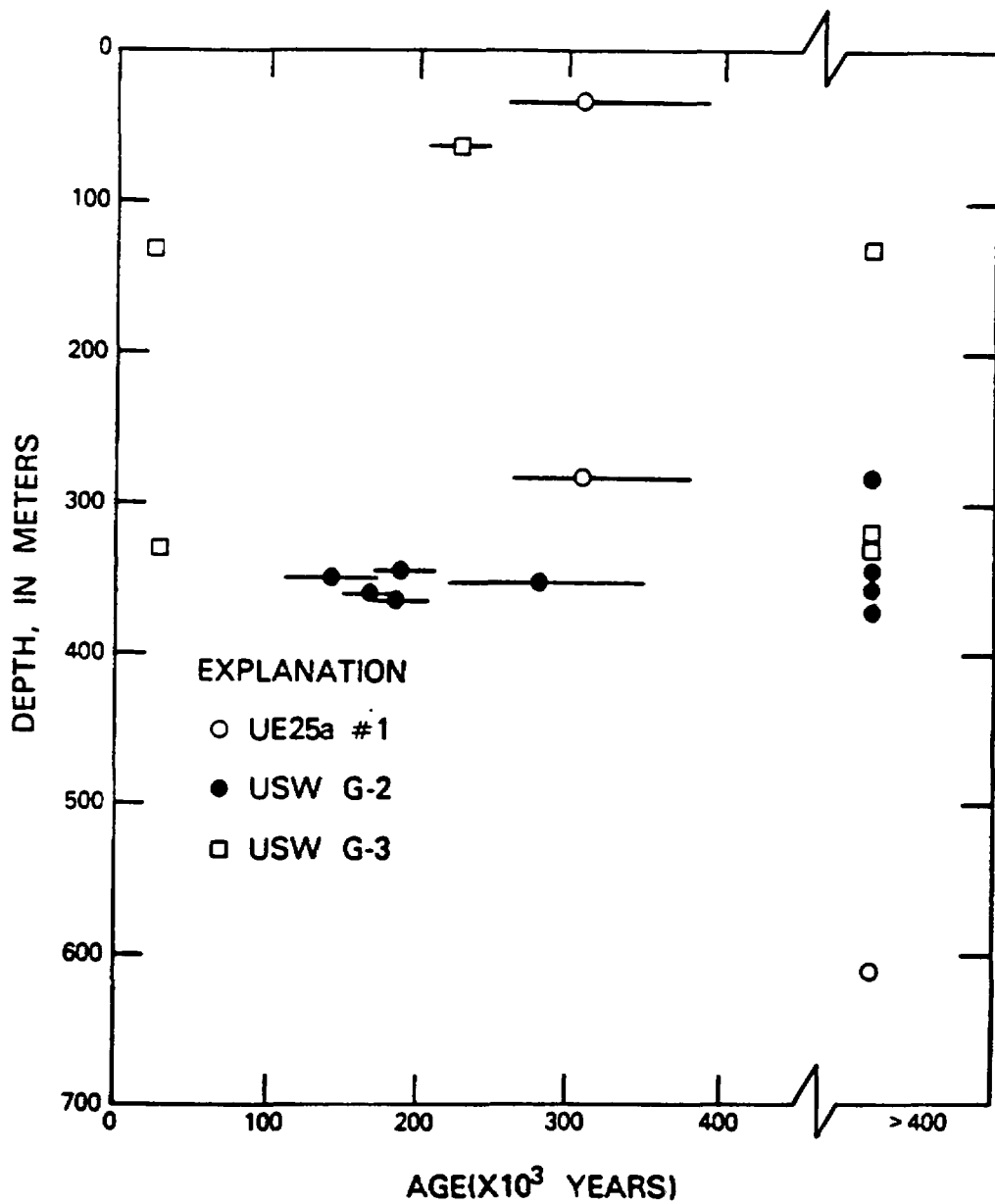


Figure 3. Calculated uranium-series dates ($\times 10^3$ years) of fracture and cavity filling calcite and opal in drill holes area plotted against corresponding depths in meters. Bars indicate experimental errors.

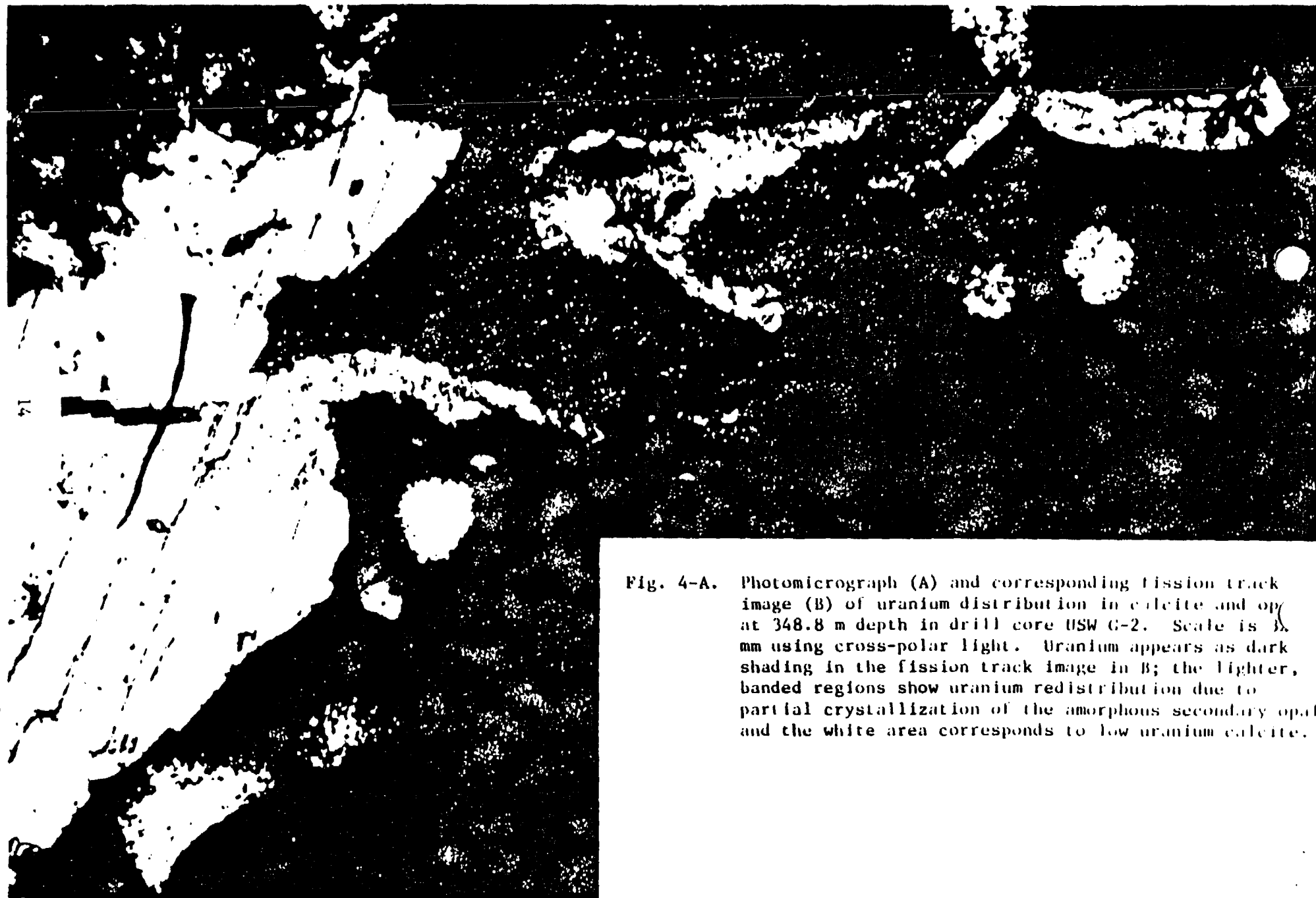


Fig. 4-A. Photomicrograph (A) and corresponding fission track image (B) of uranium distribution in calcite and opal at 348.8 m depth in drill core USW G-2. Scale is 0.5 mm using cross-polar light. Uranium appears as dark shading in the fission track image in B; the lighter, banded regions show uranium redistribution due to partial crystallization of the amorphous secondary opal and the white area corresponds to low uranium calcite.



FIG. 4-B.

opal (57.8 ppm U-sample 343.8-3, table 2) confirms that nearly all uranium is in the silica phase. However, significant amounts of uranium may be lost from the amorphous opal by the process of crystallization.

Examination of the stable isotopic composition of calcites reveals no obvious correlation between the $\delta^{18}\text{O}$ values and dates obtained for the samples. The absence of such a correlation indicates that the samples have not been subjected to systematic diagenesis or that significant change with time in the isotopic composition of the fluids which precipitated the calcite had not occurred. Also because the isotopic composition of the fluids did not apparently change with time, the $\delta^{18}\text{O}$ value of the calcites can be used to constrain the isotopic composition and the origin of the fluid. The difference in $\delta^{18}\text{O}$ values of co-existing calcite and water at 20°C is about 30 per mil (O'Neil and others, 1969) so that the water in equilibrium at this temperature with the shallowest calcites with $\delta^{18}\text{O}$ of about +20 (fig. 5) would have $\delta^{18}\text{O}$ values near -10. This value is normal of modern meteoric water of this area and suggests that the source for the oxygen in these fracture-filling calcites is meteoric water. The fluids which precipitated the deeper, more ^{18}O -depleted calcites (fig. 5), had either lower $\delta^{18}\text{O}$ values or experienced higher temperatures than those which equilibrated with the shallow samples.

The $\delta^{13}\text{C}$ values in drill core calcites of the Yucca Mountain range between about -4 and -8 (fig. 6). There are two probable sources for the carbon in these secondary calcites. One source is dissolved atmospheric CO_2 in the groundwaters which would produce $\delta^{13}\text{C}$ values near -1 in carbonates similar to those from the nearby Amargosa Desert (Kyser and others, 1981). The other source is reduced carbon from either organic matter or from the tuffs themselves; the $\delta^{13}\text{C}$ value of these sources may approach -20. The $\delta^{13}\text{C}$

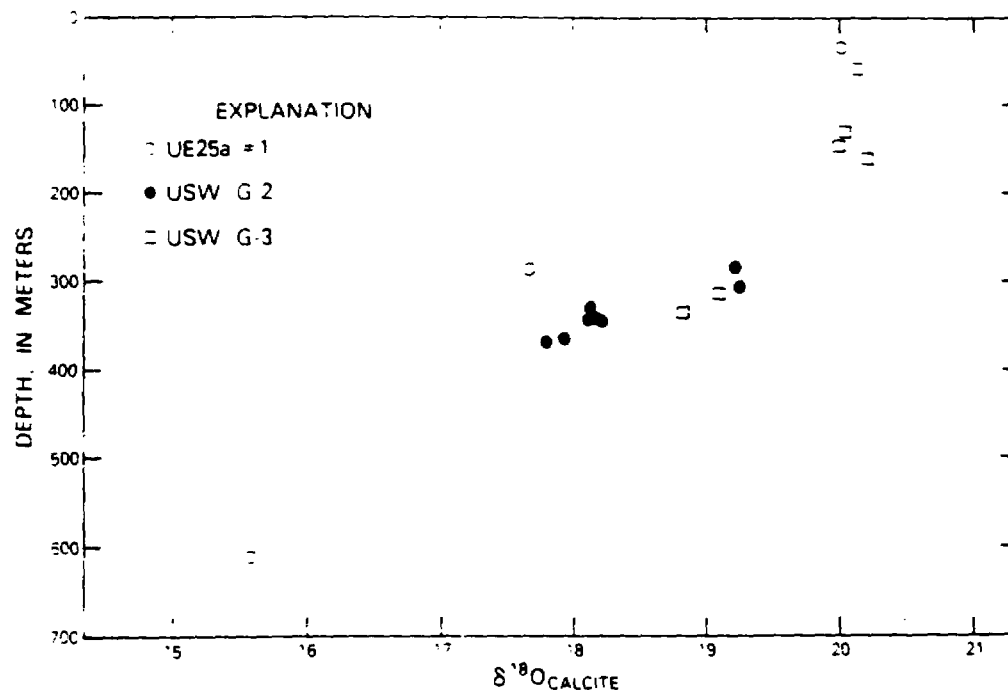


Figure 5. $\delta^{18}\text{O}$ values of calcite from drill holes and surface travertines are plotted against depth of sample.

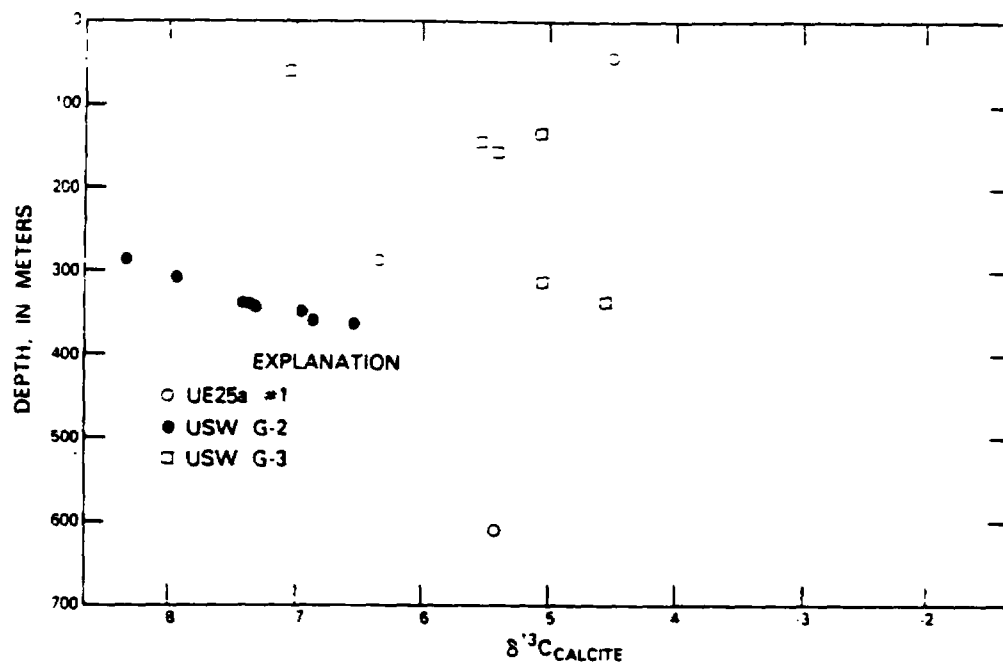


Figure 6. Relationship between the $\delta^{13}\text{C}$ value and depth of calcite from the Yucca Mountain area.

values of -4 to -8 per mil suggest that most of the carbon comes from dissolved atmospheric CO₂.

The $\delta^{18}\text{O}$ values decrease consistently with depth in all three drill holes (fig. 5). In contrast, the $\delta^{13}\text{C}$ values of calcites increase with depth (fig. 6). However, samples from drill holes USW G-3 have higher ^{13}C values than do those from USW G-2 at similar depths and the $\delta^{13}\text{C}$ values of drill hole UE25a#1 do not fit well the trends of the other drill holes even if $\delta^{13}\text{C}$ result of the shallowest sample (34 m, table 1) is disregarded. The general decrease of $\delta^{18}\text{O}$ and increase of $\delta^{13}\text{C}$ with depth of the calcites may result from several processes including (1) enrichment of ^{18}O and ^{12}C in the fluids which produced the shallowest samples through evaporation of ^{18}O -poor water and loss of ^{13}C -rich CO₂ from ascending deeper fluids, (2) depletion of ^{18}O and ^{12}C in the deeper fluids as a result of continued precipitation of calcite, (3) production of each calcite from fluids having different origins, and (4) increase in the temperature of precipitation of calcite with depth as the same fluid responds to the local geotherm.

Although the climate of the Yucca Mountain area is conducive to evaporation at the surface, the regular decrease in the $\delta^{18}\text{O}$ values of the calcites to depths of several hundred meters in conjunction with the high degrees of evaporation (>50%) needed to produce the required appropriate isotopic modification of the deep fluid suggests that this mechanism is unlikely. Similarly, the quantity of calcite that would have to precipitate from the shallow fluids to produce the appropriate $\delta^{18}\text{O}$ values of the deeper fluids should produce much greater variation of the $\delta^{13}\text{C}$ values than is observed. The regular increase in the $\delta^{18}\text{O}$ and decrease in the $\delta^{13}\text{C}$ values of the calcites with depth argue against distinct fluids for each calcite.

The isotopic fractionation in response to increasing temperature appears to best explain the depth-related trends in the stable isotope data of the calcites in these drill holes. Using the oxygen isotope fractionation factor between calcite and water as reported by O'Neill and others (1969) and assuming a $\delta^{18}\text{O}$ value for meteoric water of -9, the measured $\delta^{18}\text{O}$ values of the Yucca Mountain calcites suggest equilibration temperatures at about 20°C near the surface and at about 46°C for the sample at a depth of 611 meters (fig. 7). The corresponding enrichment of ^{13}C with depth in calcites from the same drill holes can also be explained by increasing the temperature at which the calcite precipitates. These estimates of the changes of temperature with depth correspond to a maximum geothermal gradient of 43°/km. This value represents an upper limit of the gradient because the descending meteoric water can also become ^{18}O -depleted and ^{13}C -enriched as a result of the precipitation of the carbonate.

Sass and others (1980) estimated thermal gradients of about 36°/km for depths to 470 meters in hole UE25a#1 and mean annual ground-surface temperatures of 14.8°C. A gradient of 45°/km was estimated for another hole (UE25a#3) about 12 km from UE25a#1 (Sass and others, 1980). These gradients agree well with that estimated from the isotopic composition of calcite in the drill holes although we assumed a surface temperature of precipitation of the calcite of about 20°C. Sass and Lachenbruch (1982) also report the possible downward percolation of ground water through both unsaturated and saturated zones at a rate on the order of 1 to 10 mm/year in the Yucca Mountain area. The stable isotope data presented here suggest that meteoric water moved downward from the surface along fractures and precipitated calcite in near equilibrium with the geotherm.

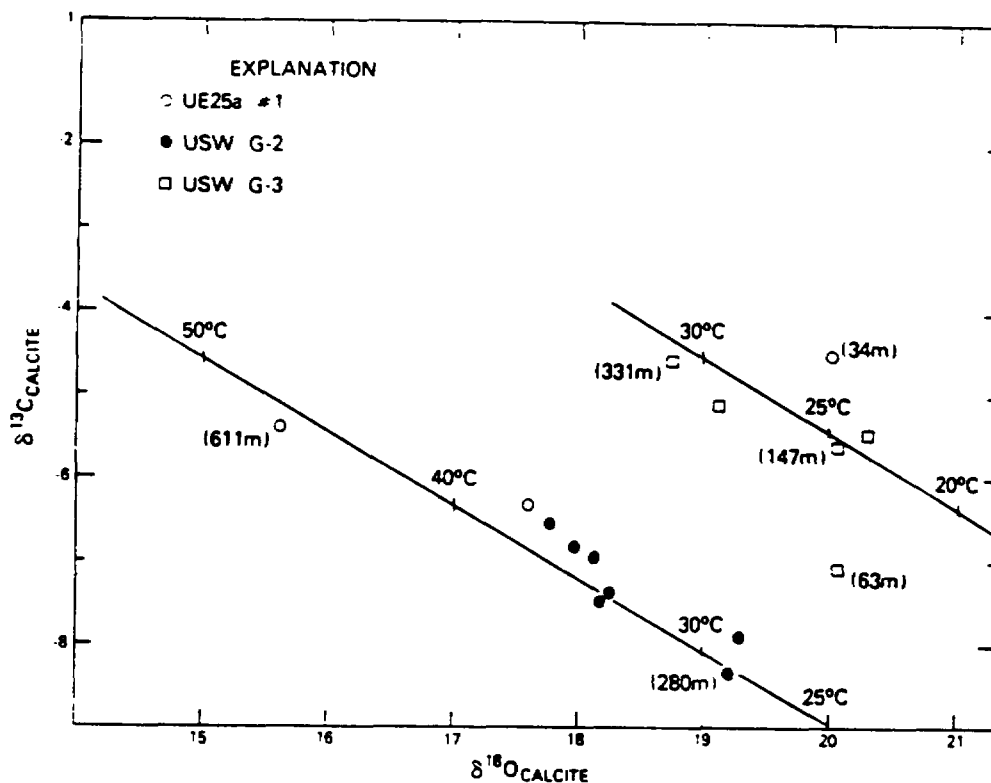


Figure 7. $\delta^{18}\text{O}$ versus the $\delta^{13}\text{C}$ values of calcite from Yucca Mountain. Lines and temperatures represent the calculated isotopic composition of calcite in equilibrium with meteoric water having a $\delta^{18}\text{O}$ value of -9 and $\delta^{13}\text{C}$ values of either -11.5 (lower line, hole USW G-2) or -8 (upper line, hole USW G-3). Fractionation factors for oxygen are those suggested by O'Neill and others (1969) and for carbon are those derived by Friedman 1970). The depth of some of the samples in meters are indicated in parentheses.

SUMMARY

Stable isotope data indicate that fracture and cavity filling calcite in Yucca Mountain drill cores precipitated from downward migrating meteoric water. The observed decrease in $\delta^{18}\text{O}$ and increase in $\delta^{13}\text{C}$ contents of calcite deposits with respect to depth (fig. 7) are interpreted as being primarily due to increase in temperature of the water moving downward along fractures in the unsaturated zone. The changes of temperature with depth, deduced from measured $\delta^{18}\text{O}$ values, correspond to a maximum geothermal gradient of $43^\circ/\text{km}$.

The percolating ground water leached uranium and other elements from wall-rocks becoming saturated with respect to calcite and silica. Subsequently, various amounts of dissolved uranium coprecipitated with calcite and opal. Some of these deposits in three drill holes were selected for dating by the uranium-series method. All dates are calculated by assuming a closed system, and single generation with rapid rates of accumulation of the fracture filling deposits. Of the eighteen samples dated, four calcite deposits and all four of the opal deposits are older than the detection limit of the method of about 400,000 years, and ten calcite deposits yield dates between 26,000 and 310,000 years (table 4). The finite dates of precipitation indicate fluid movement and fracture filling during the last 310,000 years.

Generalizing on a limited data base, the migration of meteoric water and subsequent calcite precipitation are probably tectonically controlled. Fractures caused by tectonic processes allowed ground water to move until the openings became obstructed by precipitating calcite. The obtained dates for calcite precipitation are then minimum ages for tectonic episodes. Another possible interpretation of the results is that water migration and calcite precipitation were climatically regulated. That is, ground water movement and calcite formation occurred during period of high rainfall. Three groups of

calcite dates may be recognized from our data which may correspond to pluvial periods at the Yucca Mountain area: two calcite deposits yield an average date of 28,000 years, four calcite deposits yield an average date of about 170,000 years, and the average date of four other calcite deposits is about 280,000 years (fig. 3). Alternatively, the finite calcite dates may be the result of open-system modification. In this explanation, all calcite deposits are presumed to be older than 400,000 years. Crystallization of opal then released additional uranium which was incorporated in some of the calcite deposits making them to appear too young. As presented in fig. 4-B, crystallized opal coexisting with calcite exhibits uranium redistribution and possibly uranium loss as a function of recrystallization, but there is no indication of secondary uranium uptake by the lowest-uranium containing host calcite (sample 348.8-A in table 2).

In conclusion, this preliminary investigation of calcite and opal deposits in fractures of Yucca Mountain drill cores combining uranium-series dating and stable isotope data show promise to warrant a more systematic sampling. Refinements of the procedure in a future study should include identification of possible multiple generation of calcite, determination of relationship between coexisting calcite and opal, and searching for evidence of secondary uranium migration by using thin-sections, luminescence observations and fission-track radiography.

ACKNOWLEDGEMENTS

Samples were provided by R. B. Scott, W. J. Carr and R. W. Spengler. The paper benefited from review comments by R. B. Scott and R. A. Zielinski. We thank R. A. Zielinski for providing the photomicrograph and fission track images.

REFERENCES

- Friedman, I., 1970, Some investigations of the deposition of travertine from Hot Springs-I. The isotopic chemistry of a travertine-depositing spring: *Geochimica et Cosmochimica Acta*, v. 34, p. 1303-1315.
- Kyser, T. K., Hay, R. L., and Teague, T. T., 1981, Isotopic composition of carbonates and clays in the Amargosa Desert, Nevada and California: *Geological Society of America, Abstracts with Programs*, v. 13, p. 492.
- Hagstrum, J. T., Daniels, J. J., and Scott, J. H., 1980, Interpretation of geophysical well-log measurements in drill hole UE25a-1, Nevada Test Site, Radioactive Waste Program: U.S. Geological Survey Open-File Report 80-941, 32 p.
- Maldonado, F., and Koether, S. L., 1983, Stratigraphy, structure, and some petrographic features of Tertiary volcanic rocks at the USW G-2 drill hole, Yucca Mountain, Nye County, Nevada: U.S. Geological Survey Open-File Report 83-732, 83 p.
- O'Neil, J. R., Clayton, R. N., and Mayeda, T. K., 1969, Oxygen isotope fractionation in divalent metal carbonates: *Journal Chemical Physics*, v. 51, p. 5547-5558.
- Sass, J. H., and Lachenbruch, A. H., 1982, Preliminary interpretation of thermal data from the Nevada Test Site: U.S. Geological Survey Open-File Report 82-973, 30 p.
- Sass, J. H., Lachenbruch, A. H., and Mase, C. W., 1980, Analysis of thermal data from drill holes UE25a-3 and UE25a-1, Calico Hills and Yucca Mountain, Nevada Test Site: U.S. Geological Survey Open-File Report 80-826, 25 p.

- Scott, R. B., and Castellanos, M., 1984, Stratigraphic and structural relations of volcanic rocks in drill holes USW GU3 and USW G-3, Yucca Mountain, Nye County, Nevada: U.S. Geological Survey Open-File Report 84-491, 121 p.
- Szabo, B. J., Carr, W. J., and Gottschall, W. C., 1981, Uranium-thorium dating of Quaternary carbonate accumulations in the Nevada Test Site region, southern Nevada: U.S. Geological Survey Open-File Report 81-119, 35 p.
- Szabo, B. J., and Rosholt, J. N., 1982, Surficial continental sediments, in Ivanovich, M. and Harmon, R. S., eds., Uranium-series disequilibrium: Applications to environmental problems: New York, Oxford University Press, p. 246-267.

ENCLOSURE 3

52ABO

2974

NATURAL RADIOCARBON, SOLAR ACTIVITY,
AND CLIMATEFROM USES-OFR-
78-701

By Hans E. Suess
University of California, San Diego
Department of Chemistry
La Jolla, California 92093

A power spectrum of the natural atmospheric carbon-14 variations since 5400 B.C. reveals a very distinct cycle with a period of 203 years. This period was particularly pronounced during sub-Atlantic times since about 800 B.C. It is also very marked for the time prior to 3400 B.C., the so-called Atlantic period. The time

of the Subboreal shows a markedly different power spectrum, indicating a correlation between carbon-14 variations and climate. During sub-Atlantic and Atlantic times, the 200 year cycle is in phase and is so regular that the clock governing this periodicity can be assumed to be in the sun.

DATING CALICHES FROM SOUTHERN NEVADA
BY $^{230}\text{Th}/^{232}\text{Th}$ VERSUS $^{234}\text{U}/^{238}\text{U}$
AND $^{230}\text{Th}/^{234}\text{U}$ VERSUS $^{234}\text{U}/^{238}\text{U}$
ISOTHERM-PLLOT METHOD

230TH/232TH VERSUS
234U/232TH AND
234U/232TH VERSUS
238U/232TH

By Barney J. Szabo and Horst Stier
U.S. Geological Survey
Denver Federal Center
Denver, Colorado 80225
University of Colorado
Boulder, Colorado 80304

Caliches are widespread components in most of the world's dry zones. Dating these deposits is important because it would help to assess paleoclimatic conditions, it would allow us to understand the geomorphic processes affecting pediments and river terraces, and it would play a significant role in studies of Quaternary faulting.

Inorganically precipitated carbonates, such as caliches, may be dated by the uranium-series method, provided that the samples initially had uranium but no thorium isotopes and that the samples were free of post-depositional migration of uranium and its long-lived daughter isotope ^{230}Th . The major problem with dating caliches is that they always contain large amounts of detrital materials that cannot be separated from the carbonate fraction by simple physical means.

Because of the difficulties involved, there are few published data on dating caliches. Ku (oral commun., 1975) and Ku and others (1977) reported on dating on soil caliches. They leached the samples with dilute hydrochloric acid and analyzed both soluble and insoluble fractions. Ages were calculated from the results of the soluble fraction after correcting for chemical fractionations. Rosholt (1976) dated caliche rinds and travertines. The samples were ashed to CaO and the soluble and

insoluble fractions of individual aliquots were separated by means of dilute acetic, nitric and hydrochloric acids. The ages were calculated using $^{230}\text{Th}/^{232}\text{Th}$ versus $^{234}\text{U}/^{232}\text{Th}$ plots of the soluble and insoluble fractions. It was shown that the use of dilute nitric acid produced the least chemical fractionation. Szabo and Butzer (in press) analyzed caliches from playa deposits. They dissolved and analyzed an aliquot of the total sample; then another aliquot was leached by dilute acetic acid and the acid insoluble residue was also analyzed. Ages were calculated from the $^{230}\text{Th}/^{234}\text{U}$ versus $^{232}\text{Th}/^{232}\text{U}$ and $^{234}\text{U}/^{238}\text{U}$ versus $^{230}\text{Th}/^{238}\text{U}$ plots.

Samples for this study were crushed, ground to a fine powder, then ashed for a period of about eight hours at 900°C to convert all CaCO_3 to CaO . Each sample was added to a dilute solution of nitric acid (0.1-0.5 N HNO_3) in very small portions so that at no time was the solution allowed to turn basic. The final acidity of the solution, with the slurry of the detrital acid-insoluble component, was set to about pH 1. The liquid and solid fractions were separated by centrifuge and the solid fraction was dried and weighed. Both fractions were then spiked by a combined solution of ^{235}U , ^{230}Th , and ^{232}Th .

The acid-insoluble residue was totally dissolved by repeated addition of concentrated HClO₄, HNO₃ and HF mixtures. The uranium and thorium in the acid-soluble fraction were coprecipitated with iron and aluminum hydroxides by the addition of concentrated NH₄OH. The precipitate was separated by centrifuge, dissolved in 6N HNO₃, and loaded on an anion-exchange resin column in NO₃⁻ form. Further steps of purification and separation were described previously by Szabo and Rosholt (1969). The uranium and thorium concentrations, ²³⁸U/²³⁵U, ²³²Th/²³⁰Th and ²³²Th/²³⁰U were determined by alpha-spectrometry (Rosholt and others, 1966).

Results of the analyses and calculated ages of six caliche samples (both soluble and insoluble fractions) from southern Nevada localities are shown in table 1. Ages are calculated by means of isochron plots of the

respective acid-soluble and acid-insoluble residue pairs. The slope of the ²³²Th/²³⁰Th versus ²³⁸U/²³⁵U plot yields the ²³²Th/²³⁰U activity ratio of the pure carbonate component. The slope of the ²³²Th/²³⁰Th versus ²³⁸U/²³⁵U yields the ²³²Th/²³⁰U activity ratio of the pure carbonate component. From these isotopic ratios isochron-plot ages of the caliches are calculated using the standard radioactive decay and growth equations.

Sample no. 60 is a thick caliche rind between cobbles that was collected from a caliche-cemented colluvium near Lathrop Wells by W. J. Carr. Dating this sample is particularly interesting because the deposit is directly overlain by a basalt flow dated 250,000 ± 50,000 years by whole-rock K-Ar method. (W. J. Carr, U.S.G.S., written commun.). Sample no. 60-A is the inner laminated, dense zone.

Table 1.--Uranium-series data and isochron-plot ages of caliche samples

[SOLN, acid-soluble solution; RES, acid-insoluble residue.]

Sample No.	Fraction	U (ppm)	²³² Th/ ²³⁰ Th	²³⁸ U/ ²³⁵ U	²³² Th/ ²³⁰ U	U-series isochron-plot age (years)
60-A	SOLN	5.32 ± 0.32	6.98 ± 0.28	1.23 ± 0.02	1.35 ± 0.04	345,000 ± 180,000
	RES	3.73 ± 0.56	1.46 ± 0.06	1.06 ± 0.02	1.34 ± 0.05	70,000
60-B	SOLN	5.37 ± 0.08	5.62 ± 0.22	1.20 ± 0.02	1.33 ± 0.04	400,000
	RES	6.11 ± 0.09	1.62 ± 0.06	1.10 ± 0.02	1.04 ± 0.04	--
50	SOLN	6.21 ± 0.09	11.2 ± 0.2	1.37 ± 0.02	0.242 ± 0.010	24,000 ± 3,000
	RES	4.36 ± 0.07	4.56 ± 0.12	1.34 ± 0.02	0.279 ± 0.011	--
51	SOLN	4.77 ± 0.07	1.62 ± 0.65	1.37 ± 0.02	0.164 ± 0.007	8,000 ± 2,000
	RES	3.50 ± 0.35	1.07 ± 0.04	1.20 ± 0.02	0.587 ± 0.023	--
NOV-1	SOLN	6.51 ± 0.13	2.95 ± 0.12	1.21 ± 0.02	0.827 ± 0.035	129,000 ± 20,000
	RES	4.09 ± 0.06	1.37 ± 0.05	1.10 ± 0.02	1.1 ± 0.05	--
NOV-2	SOLN	16.8 ± 0.3	2.90 ± 0.35	1.34 ± 0.02	0.040 ± 0.0032	4,000 ± 2,000
	RES	11.4 ± 0.2	1.82 ± 0.09	1.35 ± 0.02	0.331 ± 0.013	--

1 The inner part of the hard and dense caliche rind growing on cobbles from caliche-cemented colluvium near Lathrop Wells; collected by W. J. Carr.

The softer and porous outer part of the same caliche rind as .

Poorly cemented, porous caliche filling along recent fault; collected at the Oak Spring area by W. J. Carr.

Strongly cemented, porous caliche in Cca horizon; collected at the Oak Spring area by W. J. Carr.

Soft, powdery caliche collected at the base of a trench in pediment gravel at Lyncline Ridge area; collected by H. Morrison and A. Bernard.

Hard caliche layer from the inner part of the same trench as .

Sample no. 60-B is the outer, softer, and porous part of the same caliche rind. The isochron-plot age of sample no. 60-A is 345,000 \pm 30,000 years, and is in good agreement with the limiting K-Ar age of the basalt flow. It appears from the isotopic date of sample no. 60-B that some extraneous Th was taken up by this sample late in its geologic history, probably while the old colluvium was being down-cut by modern drainage. The approximate age estimate for this sample is 400,000 years or about the same age as sample no. 60-A, as expected.

Sample no. 50 and no. 51 were collected at the Oak Springs area by M. J. Carr. The poorly cemented, porous caliche is filling along recent fault. The well-cemented but porous caliche sample no. 51, from the Cca horizon is judged on topographic and morphologic considerations to be relatively young in age. The isochron-plot ages of samples no. 50 and no. 51 are 24,000 \pm 3000 and 8000 \pm 2000 years, respectively.

Samples no. Nov-1 and no. Nov-2 are from a trench in pediment gravel overlying the Eleana Formation of Mississippian age in the Syncline Ridge area. The trench was sampled and mapped by D. Hoover and A. Fernard, U.S.G.S. Sample no. Nov-1 is from a soft, powdery caliche layer at the base of the trench. The isochron-plot age of this sample is 128,000 \pm 20,000 years and the pediment

gravel must be at least that old. Sample no. Nov-2 is from a hard caliche layer at the upper part of the trench. This hard caliche shows evidence of redeposition, therefore the isochron-plot age of 4000 \pm 2000 years is probably a minimum-age estimate only.

- Ku, T. L., Bull, W. B., Freeman, S. T., and Knauss, K. G., 1977. Th/U dating of pedogenic carbonates in desert soils: Geological Society of America Abstracts with Programs, v. 9, no. 7, p. 1061.
- Rosholt, J. N., 1976. Th/U dating of travertine and caliche rinds: Geological Society of America Abstracts with Programs, v. 8, no. 6, p. 1076.
- Rosholt, J. N., Doe, B. R., and Tatsumoto, M., 1966. Evolution of the isotopic composition of uranium and thorium in soil profiles: Geological Society of America Bulletin, v. 77, no. 9, p. 987-1004.
- Szabo, B. J., and Butzer, K. W., (in press). Uranium-series dating of lacustrine limestones from pan deposits with final Acheulian assemblage at Rooibad, Kimberley District, South Africa.
- Szabo, B. J., and Rosholt, J. N., 1969. Uranium-series dating of Pleistocene molluscan shells from southern California - An open system model: Journal of Geophysical Research, v. 74, no. 12, p. 3253-3260.

RARE GAS ELEMENTAL ABUNDANCES AND ISOTOPIC COMPOSITIONS IN DIAMONDS

By N. Takaoka¹ and M. Ozima²

¹Department of Physics, Osaka University
Toyonaka 560, Japan

²Geophysical Institute, University of Tokyo
Tokyo 113, Japan

The rare gases have been extracted from natural diamonds in a three-step heating program, at 800°C, 2000°C and 2100°C. Elemental abundances and isotopic compositions of the extracted rare gases were studied using a mass spectrometer.

Samples: Experiments have been conducted in two phases. For the first phase, about 6 grams of industrial diamonds were purchased. Two years later, about 5 grams of industrial diamonds were purchased from the same dealer. We were told by the dealer that both groups of diamonds came from the Kimberley Mines, South Africa. There seemed no visible difference between the two groups of diamonds. They are about 4 mm in size, some have visible black inclusions, and some are nearly inclusion-free.

In the first phase of the experiment, dia-

monds were divided by eye into two batches (the nearly inclusion-free and the inclusion-rich) purely on the basis of the amount of inclusions. To facilitate degassing, both batches of diamonds were crushed in a stainless steel mortar with a stainless steel burin and a hammer. The crushed sample ranged from a few hundred micrometers to a few millimeters. No attempt was made to separate the inclusions from the crushed diamonds. Rare gas extraction was made on the crushed samples.

In the second phase of the experiment, diamonds were first crushed to less than a few hundred microns. The crushed samples were then divided into two batches (the nearly inclusion-free and the inclusion-rich). The nearly inclusion-free sample was kept in hot HNO₃ overnight to remove any inclusions and contaminations that

13. Water-Table Decline in the South-Central Great Basin During the Quaternary: Implications for Toxic Waste Disposal

By Isaac J. Winograd and Barney J. Szabo

CONTENTS

Abstract	147
Introduction	147
Acknowledgments	148
Rates of apparent water-table decline	148
Discussion and synthesis	150
Implications for toxic waste disposal	151
References cited	152

Abstract

The distribution of vein calcite, tufa, and other features indicative of paleo-ground-water discharge indicates that during the early and middle Pleistocene the water table at Ash Meadows, in the Amargosa Desert, Nevada, and at Furnace Creek Wash, in east-central Death Valley, California, was tens to hundreds of meters above the modern water table, and that ground-water discharge occurred up to 18 km up the hydraulic gradient from modern discharge areas. Uranium-series dating of the calcitic veins permits calculation of rates of apparent water-table decline; rates of 0.02 to 0.08 m/ka are indicated for Ash Meadows and 0.2 to 0.6 m/ka for Furnace Creek Wash. The rates for Furnace Creek Wash closely match a published estimate of vertical crustal offset for this area, suggesting that tectonism is a major cause for the displacement observed. In general, displacements of the paleo water table probably reflect a combination of (1) tectonic uplift of vein calcite and tufa, unaccompanied by a change in water-table altitude, (2) decline in water-table altitude in response to tectonic depression of areas adjacent to dated veins and associated tufa, (3) decline in water-table altitude in response to increasing aridity caused by major uplift of the Sierra Nevada and Transverse Ranges during the Quaternary, and (4) decline in water-table altitude in response to erosion triggered by increasing aridity and (or) tectonism.

A synthesis of hydrogeologic, neotectonic, and paleo-climatologic information with the vein-calcite data permits the inference that the water table in the south-central Great Basin progressively lowered throughout the Quaternary. This inference is pertinent to an evaluation of the utility of thick (200–600 m) unsaturated zones of the region for isolating solidified radioactive wastes from the hydrosphere for hundreds of millenia. Wastes buried a few tens to perhaps 100 m above the modern water table—that is above possible water level rises due to future pluvial

climates—are unlikely to be inundated by a rising water table in the foreseeable geologic future.

INTRODUCTION

Regional interbasin flow of ground water through the thick section of Paleozoic carbonate rocks of the south-central Great Basin has been the subject of numerous studies in the past 25 years (Hunt and Robinson, 1960; Loeltz, 1960; Winograd, 1962; Winograd and Thordarson, 1968; Winograd, 1971; Winograd and Friedman, 1972; Naff, 1973; Winograd and Thordarson, 1975; Dudley and Larson, 1976; Winograd and Pearson, 1976; Waddell, 1982). Flow through the regional carbonate-rock aquifer is directed toward major spring discharge areas at Ash Meadows in the Amargosa Desert of Nevada and toward Furnace Creek Wash in east-central Death Valley, California (fig. 13.1). The flow occurs under hydraulic gradients as low as 0.06 m/km (Winograd and Thordarson, 1975, pl. I), reflecting the high fracture transmissivity of this aquifer. Locally, major hydraulic barriers compartmentalize the aquifer (Winograd and Thordarson, 1968, 1975). A detailed hydrogeologic and hydrogeochemical synthesis of this vast flow system, including potentiometric maps, is available in Winograd and Thordarson (1975).

A variety of geologic evidence indicates that during the Pleistocene the water table in the regional carbonate-rock aquifer at Ash Meadows and at Furnace Creek Wash (fig. 13.1) was tens to hundreds of meters above the modern water table (Winograd and Doty, 1980). The evidence consists of tufas; ancient spring orifices; calcitic veins and cylindrical calcite-lined tubes that mark the routes of paleo ground water flow to spring orifices; and paleo water levels inscribed on the walls of Devils Hole (fig. 13.1), a fault-controlled collapse feature adjacent to the Ash Meadows discharge area. Most of these have been briefly described elsewhere (Winograd and Thordarson, 1975, p. C82–C83; Winograd and Doty, 1980; Pexton, 1984; Winograd and others, 1985). In this study we focus on the calcitic veins as indicators of paleo water tables because they are readily datable using uranium-disequilibrium methods (Szabo and others, 1981; Winograd and others, 1985). This report is an initial step toward a quantification of the observations of Winograd and Doty (1980).

Acknowledgments

We thank D. Stuart-Alexander, W.J. Carr, W.W. Dudley, Jr., W.R. Osterkamp, N.J. Trask, Jr., R.B. Scott, and W.E. Wilson for helpful review comments, and we appreciate the excellent assistance provided by G.C. Doty and A.C. Riggs during the field search for the calcitic veins.

RATES OF APPARENT WATER-TABLE DECLINE

At Ash Meadows, the calcitic veins occur in association with, and adjacent to, a structurally controlled 16-km-long spring discharge area (Winograd and Thordarson, 1975). The veins occur as much as 50 m higher than and

as much as 14 km up the hydraulic gradient from the highest water level (altitude 719 m) at Ash Meadows—namely, that in Devils Hole (Winograd and Doty, 1980). Veins AM-7, DH-1, and AM-10 from Ash Meadows and northern Amargosa Flat (fig. 13.1) are, respectively, 11, 19, and 26 m higher than the water level in Devils Hole (table 13.1). (The hydraulic gradient in the region between these veins is extremely small—0.06 m/km (Winograd and Thordarson, 1975, pl. D)—so that for practical purposes the altitude of the veins can be compared directly to the water level in Devils Hole.) Uranium-disequilibrium dating of these veins yields an age of 510 ± 62 ka for the youngest laminae in vein AM-7, 660 ± 75 ka for the youngest laminae in vein DH-1, and 750 ± 52 ka for the center of vein AM-10 (table 13.1). These data permit calculation of the average rates of apparent water-

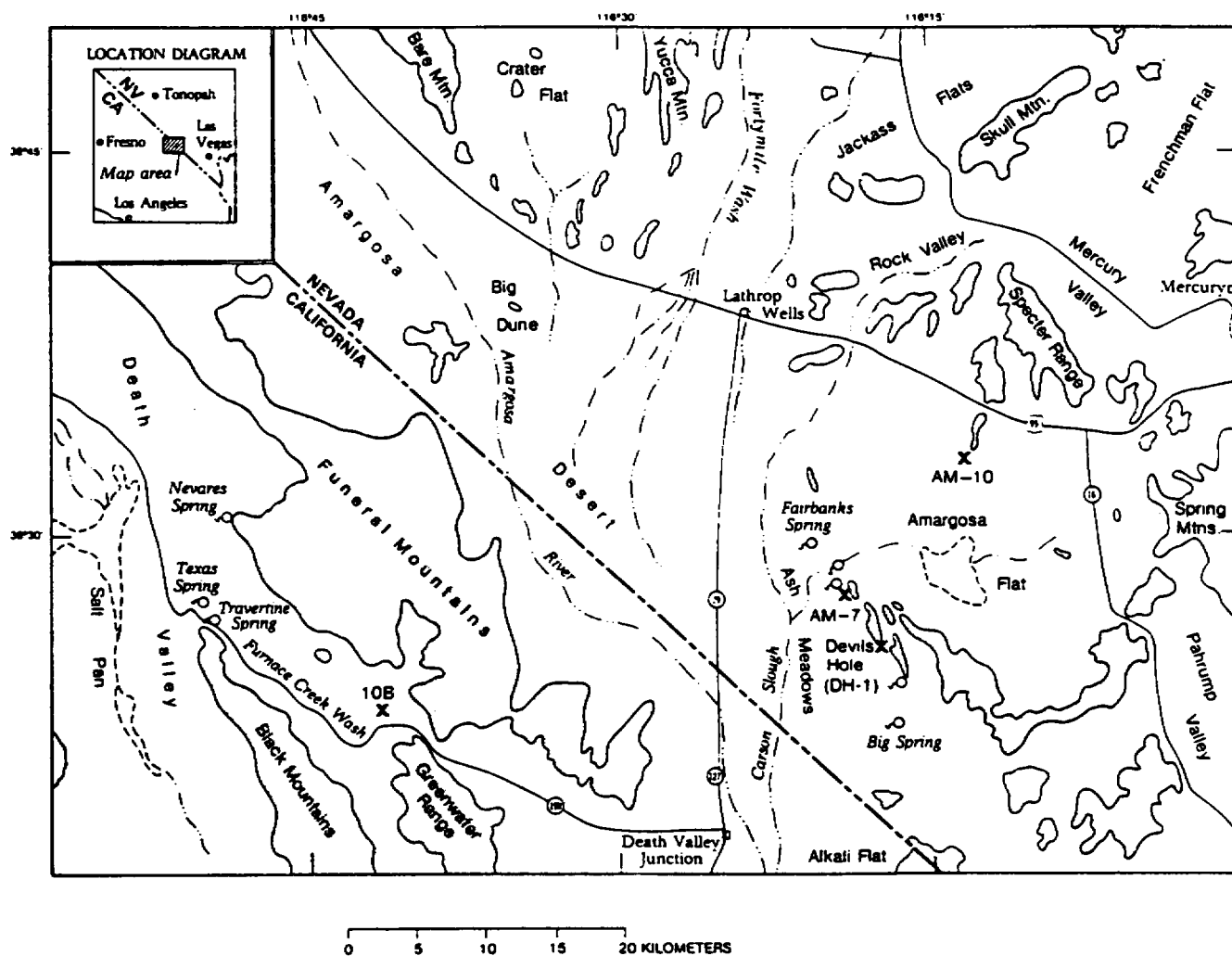


Figure 13.1. Index map of south-central Great Basin, Nevada-California. Uplands shaded; x's mark location of uranium-series dated calcitic veins discussed in text.

table decline; rates on the order 0.02 to 0.03 m/ka are indicated (table 13.1). These rates are minimum values, first, because we do not know how high above outcrop the sampled veins might have extended prior to erosion; and second, because the youngest laminae in our veins may only record the time of sealing of the vein, rather than the time of cessation of ground-water discharge. Nevertheless, because the numerator (that is the altitude difference between vein outcrop and water level in Devils Hole) in our ratio is so much smaller than the denominator (vein age), any reasonable combination of values yields a very slow rate of decline. For example, if the altitude of vein DH-1 were 20 m higher prior to erosion (a large value considering the present relief on the Pliocene and Pleistocene rocks in central Ash Meadows) and if ground-water discharge ceased 400 ka instead of 660 ka ago, we still calculate an apparent rate of water-table decline which is less than 0.1 m/ka.

The average rates of water-table decline cited above (0.02 to 0.03 m/ka) were calculated (table 13.1, columns 1-5) assuming a constant rate of decline during the middle and late Pleistocene, that is over times 510 to 750 ka long. A more realistic computation of decline rate is one involving three vein pairs that differ in age by only 90 to 240 ka. Such a computation (table 13.1, columns 6-7) yields rates of decline which are 2 to 2½ times as large as the average rates, namely 0.05 to 0.08 m/ka. The paired veins record ground-water flow in the period 510 ka to 750 ka (table 13.1). When these data are arranged by decreasing age and are coupled with the average rate of decline calculated for the past 510 ka (0.02 m/ka, derived from the youngest and lowest vein, AM-7, and the water-table altitude in Devils Hole), we see a suggestion of a possible reduction in rate of water-table decline during the middle Pleistocene; that is, a rate of 0.08 m/ka is indicated for the period 750 to 660 ka, a

rate of 0.05 m/ka for the period 660 to 510 ka and a rate of 0.02 m/ka for the past 510 ka. In view of the caveats presented in the preceding paragraph, additional work is clearly in order to verify the suggested change in rate of water-table decline in the Ash Meadows region. In summary, the data of table 13.1 indicate rates of apparent water decline of 0.02 to 0.08 m/ka for the Ash Meadows-Amargosa Flat area.

At Furnace Creek Wash (fig. 13.1), the rate of lowering of the water table during the Quaternary is an order of magnitude greater than the cited rates for Ash Meadows and vicinity. Here a calcitic vein swarm and associated tufa occur at an altitude of about 855 m. Uranium-disequilibrium dating of vein 10B (fig. 13.1) from this area indicates that ground-water flow in the fracture containing this vein ceased about $1,000 \pm 100$ ka. In the absence of wells or artesian springs, the water-table altitude in the regional carbonate aquifer beneath the vein swarm is unknown, but we can bracket the range of possible water-table altitudes by reference to known water levels both up and down the hydraulic gradient from the vein swarm. The altitude of the water table in the valley-fill aquifer beneath the southern Amargosa Desert, 15-20 km up the hydraulic gradient from the vein swarm, is about 640-670 m (Winograd and Thordarson, 1975, pl. 1), or about 185-215 m lower than the vein swarm (855 m). The altitude of the water table in the regional carbonate aquifer at Nevares Spring (fig. 13.1) in east-central Death Valley, 18 km down the hydraulic gradient, is 286 m or about 570 m lower than the vein swarm. (The water level at Nevares Spring is the highest level known for the regional carbonate aquifer in east-central Death Valley.) Due to the extreme aridity of the region, plus the high transmissivity of the regional carbonate aquifer (Winograd and Thordarson, 1975), the presence of a ground-water mound (a potentiometric high) in the

Table 13.1. Uranium-disequilibrium ages of calcitic veins at Ash Meadows and Amargosa Flat, Nevada, and rates of apparent water-table decline during the Quaternary

[Altitude of vein AM-10 estimated from USGS 1:24,000 Specter Range, SW topographic quadrangle; altitude DH-1 from average of four aneroid-barometer surveys. Justification for dating the calcitic veins by the $^{234}\text{U}/^{238}\text{U}$ method in Winograd and others (1985). Average rate of water-table decline assumes constant rate of decline between time of deposition of youngest laminae in vein and the Holocene; values rounded to one significant figure and represent minimum rates for reasons given in text]

Vein (see fig. 13.1 for location)	Altitude (m)	$^{234}\text{U}/^{238}\text{U}$ age (ka)	Vein altitude above water-level at Devils Hole (719 m) (m)	Average rate of water-table decline (m/ka)	Difference in altitude (m) and in youngest age (ka) for indicated vein pair	Rate of water- table decline using data of preceding column ¹ (m/ka)
AM-10-----	745±3	750±52	26±3	0.03	7, 90 (AM 10-DH 1)	0.08
DH-1-----	738	660±75 to 890±92	19	.03	15, 240 (AM 10-AM 7)	.06
AM-7-----	730±1	510±62 to 620±66	11±1	.02	8, 150 (DH 1-AM 7)	.05

¹Values rounded to one significant figure.

²Sample came from center of 1-cm-thick vein; given average growth rates (0.3 mm/ka) in other Ash Meadows veins, the time spanned during deposition of this very thin vein is unlikely to have exceeded 50 ka. (We assume the vein grew symmetrically from the walls.)

carbonate aquifer between the southern Amargosa Desert and east-central Death Valley is extremely remote; that is, we have confidence that the potentiometric surface in the carbonate aquifer beneath the vein swarm at Furnace Creek Wash is intermediate between the cited altitudes in the southern Amargosa Desert and in east-central Death Valley. The uranium-disequilibrium age, in conjunction with the cited vein and water-table altitudes, indicates an average water-table lowering of 0.2 to 0.6 m/ka.

DISCUSSION AND SYNTHESIS

Tectonics, climate change, and erosion in response to tectonics and (or) climate change are obvious potential causes for the observed water-table displacements. A comparison of the cited water-table displacement rates at Ash meadows (0.02 to 0.08 m/ka) and Furnace Creek Wash (0.2 to 0.6 m/ka) with average rates of vertical crustal offsets in these regions seemingly supports tectonism as a major cause for the displacement we have observed at Furnace Creek Wash. In east-central Death Valley, a rate of vertical crustal offset of 0.3 m/ka has been calculated by Carr (1984) for the Black Mountains (fig. 13.1) utilizing the data of Fleck (1970). In contrast, data presented by Pexton (1984, p. 49) on the displacement of a 3-m.y.-old tuff at Ash Meadows indicate relative vertical crustal offset of about 0.01 m/ka, or one-half to one-eighth of the indicated rate of water-table decline at Ash Meadows and vicinity.

Climatic change cannot be discounted as an important auxiliary cause for the documented water-table displacements. Major uplift of the Sierra Nevada and Transverse Ranges during the Pliocene and Quaternary should have markedly and progressively reduced the precipitation reaching the Great Basin during this time. Smith and others (1983, p.23) suggested that 3 m.y. ago, when the Sierra Nevada was about 950 m lower, about 50 percent more moisture might have crossed the Sierra and moved into the Great Basin. Various lines of evidence support such notions. Raven and Axelrod (1977) and Axelrod (1979), using paleobotanical evidence, argued for increasing aridity in the Great Basin, Mojave Desert, and Sonoran Desert during the late Tertiary and Quaternary. They attributed this increasing aridity to uplift of the Sierra Nevada, Transverse Ranges, Peninsular Ranges, and the Mexican Plateau. Winograd and others (1985) described a major and progressive depletion in the deuterium content of ground-water recharge in the region during the Quaternary; the most logical explanation for their data is a progressive decrease in Pacific moisture due to uplift of the Sierra Nevada and Transverse Ranges. And Pexton (1984, p. 43-46, 57), on the basis of studies of sediment depositional environments, believed that the Ash Meadows area became progressively more arid during the Quaternary.

The role of erosion in the apparent lowering of the water table is not known. We assume that in east-central

Death Valley, where the rate of vertical crustal offset is large, tectonism dominated both erosion and climate as a factor in water-table change during the Quaternary. This may not, however, be correct for the Ash Meadows region, where the rate of vertical crustal offset is an order of magnitude smaller (see above); here, the erosional history of the bordering Amargosa Desert—a history influenced by climate change and possibly also by tectonism in Death Valley—may have played an important role in the water-table changes we see at and northeast of Ash Meadows.

We should emphasize that the evidence presented by Winograd and Dory (1980), and its initial quantification herein, suggests only an apparent lowering of the water table during the Quaternary at Ash Meadows and Furnace Creek Wash. We do not know to what degree the displacement of veins and tufas relative to the modern water table reflects (1) tectonic uplift of the veins and associated tufas, unaccompanied by a decline in water-table altitude; (2) a lowering of water-table altitude in response to the tectonic downdropping of a region adjacent to the veins and tufas; (3) a lowering of water-table altitude in response to increasing aridity, or to erosion; or (4) some combination of these. Locally, uplift of the veins was probably a major cause for the displacements we observed. For example, the occurrence of the veins at Furnace Creek Wash (site 10B, fig. 13.1) at altitudes higher than the modern potentiometric surfaces to the west and east (see above) strongly suggests that major uplift of the Funeral Mountains and Greenwater Range occurred relative to both Death Valley on the west and the Amargosa Desert on the east. However, a synthesis of regional hydrogeologic, tectonic, and paleoclimatologic information with our observations indicates that a progressive and absolute lowering of the regional water table (more correctly the potentiometric surface) is likely to have occurred throughout the south-central Great Basin during the Quaternary. This inference is based on the following three considerations. (1) The several-thousand-meter topographic relief in Death Valley developed principally during the Pliocene and Pleistocene (Hunt and Mabey, 1966; U.S. Geological Survey, 1984), and the movement of the floor of Death Valley has probably been downward relative both to sea level and to bordering areas (Hunt and Mabey, 1966, p. A153). (2) Gravity-driven interbasin flow of ground water through the carbonate-rock aquifer is widespread in the region today (Winograd and Thordarson, 1975) and is directed toward Ash Meadows and Death Valley. Such interbasin flow of ground water toward Death Valley in all likelihood also occurred during the Quaternary in response to the progressive lowering of ground-water discharge outlets there. (3) The progressive increase in aridity of the region, due to uplift of the Sierra Nevada and Transverse Ranges, would presumably have resulted in a progressive reduction in ground-water recharge.

We are aware that the regional carbonate-rock aquifer is hydraulically compartmentalized by faulting (Winograd and Thordarson, 1975, p. C63-C71) and that, consequently,

the postulated lowering of ground-water base level in Death Valley during the Quaternary may not have propagated uniformly throughout the region, specifically northeast of the major hydraulic barrier at Ash Meadows (Winograd and Thordarson, 1975, p. C78-C83). Nevertheless, we believe that the combination of increasing aridity and local erosion in the Amargosa Desert during the Quaternary should, in any event, have resulted in a progressive lowering of the water table at and northeast of Ash Meadows.

Yet another mechanism for water-table lowering at and northeast of Ash Meadows that involves neither erosion nor climate change, but rather extensional fracturing, was outlined by Winograd and Doty (1980). They pointed out (p. 74-75) that the major springs at Ash Meadows oasis differ in altitude by as much as 35 m and are as much as 50 m lower than the water level in Devils Hole. Thus, periodic initiation of discharge from new spring orifices (or an increase in existing discharge) in the lower portions of this oasis due to faulting would have resulted in new and lower base levels for ground-water discharge. Implicit in their hypothesis is the belief that the faulting would be of extensional nature, opening new (or widening old) avenues of discharge from the buried Paleozoic carbonate-rock aquifer which underlies eastern Ash Meadows and which feeds all the modern springs (Winograd and Thordarson, 1975). In support of their hypothesis, we note that most of the calcitic veins in Pliocene and younger rocks at Ash Meadows strike N. $40^{\circ} \pm 10^{\circ}$ E., that is, nearly at right angles to Carr's (1974) estimate of the direction of active extension in region, namely N. 50° W. This mechanism may also have periodically lowered the water table in east-central Death Valley (fig. 13.1) where the difference in altitude between the highest (Nevares) and lowest (Texas) major springs discharging from the regional carbonate aquifer is about 170 m (Winograd and Thordarson, 1975, p. C95-C97).

Our evidence for water-table decline pertains only to the Paleozoic carbonate-rock aquifer, the "Lower carbonate aquifer" of Winograd and Thordarson (1975, table 1). As mentioned in the introduction, this regional aquifer serves as a gigantic "tile field" which integrates the flow of ground water from perhaps as many as 10 intermountain basins (Winograd and Thordarson, 1975). The water-table altitude in this regional aquifer system presently exerts a major control on the altitude of the potentiometric surface in locally overlying Cenozoic welded tuff and valley-fill aquifers (Winograd and Thordarson, 1975, p. C53-C63, and pl. I). Accordingly, we suggest further that the progressive water-table decline postulated for the regional carbonate aquifer during the Quaternary was accompanied by a decline in water-table altitude in the overlying welded tuff and valley-fill aquifers of the region.

The suggested progressive lowering of the regional water table throughout the Quaternary does not preclude superimposed and relatively rapid cyclical fluctuations in water level in response to the glacial (that is, pluvial) and interglacial climates of the Pleistocene. Indeed, preliminary

data from Devils Hole indicate that the water table in the carbonate aquifer may have fluctuated as much as 10 m in the past 30 ka (A.C. Riggs and B.J. Szabo, oral communication, December 1986). This, in turn, indicates that vein AM-7 (see above), which is only 11 m above the modern water table, would by itself be of limited utility for determination of the postulated water-table decline since the middle Pleistocene. Intensive studies of paleo water level fluctuations are underway in Devils Hole where excellent records of both Quaternary paleohydrology and paleoclimatology are preserved. We hope that these studies will permit us to distinguish between short-term (1-10 ka) and long-term (100-1,000 ka) water-table fluctuations at Ash Meadows and vicinity where the difference between the highest dated paleo water level and the highest modern water table is only 26 m (table 13.1).

IMPLICATIONS FOR TOXIC WASTE DISPOSAL

The cited evidence for an apparent lowering of the water table at Ash Meadows and Furnace Creek Wash and the inference of an absolute lowering of water table in the south-central Great Basin during the Quaternary are pertinent to an evaluation of the utility of the thick (200-600 m) unsaturated zones of the region for isolating solidified radioactive and toxic wastes from the hydrosphere for tens to hundreds of millennia (Winograd, 1981). Important information which must be obtained before using such zones for toxic waste disposal is the magnitude of water-table rise that occurred during past pluvial climates of the Pleistocene; such information would, by extension, provide clues to the likelihood of buried toxic wastes being inundated by a future rise of the water table. Winograd and Doty (1980) and Czarniecki (1985), using worst-case assumptions, suggested possible pluvial-related water-table rises of several tens of meters to 130 m above the modern water table in Frenchman Flat and beneath Yucca Mountain (fig. 13.1). As noted in the preceding section, we have preliminary information suggesting a late Wisconsin water-table rise on the order of 10 m in the carbonate aquifer at Devils Hole. Thus, it appears that solidified wastes emplaced in the thick (200-600 m) unsaturated zones of the region—at levels a few tens to a hundred meters or so above the water table—should not be inundated by a rising water table during future pluvial climates. (The depth of placement within the unsaturated zone would, of course, be chosen to preclude exhumation of the wastes by erosion.) Moreover, if our inference of a progressive lowering of water table during the Quaternary is sustained by ongoing studies of the carbonate rock and other aquifers, then it is likely that wastes buried in the unsaturated zone will in any event become increasingly displaced from the water table in the foreseeable geologic future. That is, the continuing uplift of the Sierra Nevada (Huber, 1981) and Transverse Ranges, and lowering of Death Valley (Hunt and Mabey, 1966, p. A100-A116), relative to surrounding

regions, should result in a continued progressive decline of the regional water table in the next 100,000 to 1 million yr (and beyond?) in response to increasing aridity and to lowering of ground-water base level.

REFERENCES CITED

- Axelrod, D.I., 1979, Age and origin of Sonoran Desert vegetation: California Academy of Science, Occasional Papers, no. 132, 74 p.
- Carr, W.J., 1974, Summary of tectonic and structural evidence for stress orientation at the Nevada Test Site: U.S. Geological Survey Open-File Report 74-176, 53 p.
- , 1984, Regional structural setting of Yucca Mountain, southwestern Nevada, and late Cenozoic rates of tectonic activity in part of the southwestern Great Basin, Nevada and California: U.S. Geological Survey Open-File Report 84-854, 109 p.
- Czarnecki, J.B., 1985, Simulated effects of increased recharge on the ground water flow system of Yucca Mountain and vicinity, Nevada-California: U.S. Geological Survey Water Resources Investigations Report 84-4344, 33 p.
- Dudley, W.W., Jr., and Larson, J.D., 1976, Effect of irrigation pumping on desert pupfish habitats in Ash Meadows, Nye County, Nevada: U.S. Geological Survey Professional Paper 927, 52 p.
- Fleck, R.J., 1970, Age and tectonic significance of volcanic rocks, Death Valley area, California: Geological Society of America Bulletin, v. 81, p. 2807-2816.
- Huber, N.K., 1981, Amount and timing of late Cenozoic uplift and tilt of the central Sierra Nevada, California—Evidence from the upper San Joaquin River basin: U.S. Geological Survey Professional Paper 1197, 28 p.
- Hunt, C.B., and Mabey, D.R., 1966, Stratigraphy and structure of Death Valley, California: U.S. Geological Survey Professional Paper 494-A, 162 p.
- Hunt, C.B., and Robinson, T.W., 1960, Possible interbasin circulation of ground water in the southern part of the Great Basin, in *Short papers in the geological sciences*: U.S. Geological Survey Professional Paper 400-B, p. B273-B274.
- Loeltz, O.J., 1960, Source of water issuing from springs in Ash Meadows Valley, Nye County, Nevada: Geological Society of America Bulletin, v. 71, no. 12, pt. 2, p. 1917-1918.
- Naff, R.L., 1973, Hydrogeology of the southern part of Amargosa Desert in Nevada: Reno, University of Nevada, M.S. thesis, 207 p.
- Pexton, R.E., 1984, Geology and paleohydrology of a part of the Amargosa Desert, Nevada: Berkeley, University of California, M.S. thesis.
- Raven, P.H., and Axelrod, D.I., 1977, Origin and relationships of the California flora: University of California, Publications in Botany, v. 72, 134 p.
- Smith, G.I., Barczak, V.J., Moulton, G.F., and Liddicoat, J.C., 1983, Core KM-3, a surface to bedrock record of late Cenozoic sedimentation in Searles Valley, California: U.S. Geological Survey Professional Paper 1256, 24 p.
- Szabo, B.J., Carr, W.J., and Gottschall, W.C., 1981, Uranium-thorium dating of Quaternary carbonate accumulations in the Nevada Test Site region, southern Nevada: U.S. Geological Survey Open-File Report 81-119, 33 p.
- U.S. Geological Survey, 1984, A summary of geologic studies through January 1, 1983, of a potential high-level radioactive waste repository at Yucca Mountain, southern Nye county, Nevada: U.S. Geological Survey Open-File Report 84-792.
- Waddell, R.K., 1982, Two dimensional, steady-state model of ground-water flow, Nevada Test Site and vicinity, Nevada-California: U.S. Geological Survey Water Resources Investigations Report 82-4085, 72 p.
- Winograd, I.J., 1962, Interbasin movement of ground water at the Nevada Test Site, Nevada, in *Short papers in geology and hydrology*: U.S. Geological Survey Professional Paper 450-C, p. C108-C111.
- , 1971, Origin of major springs in the Amargosa Desert of Nevada and Death Valley, California: Tucson, University of Arizona, Ph.D. dissertation, 170 p.
- , 1981, Radioactive waste disposal in thick unsaturated zones: *Science*, v.212, p. 1457-1464 (Discussion in v. 215, p. 914).
- Winograd, I.J., and Doty, G.C., 1980, Paleohydrology of the southern Great Basin with special reference to water table fluctuations beneath the Nevada Test Site during the late(?) Pleistocene: U.S. Geological Survey Open-File Report 80-569, 91 p.
- Winograd, I.J., and Friedman, Irving, 1972, Deuterium as a tracer of regional ground-water flow, southern Great Basin, Nevada-California: Geological Society of America Bulletin, v. 83, no. 12, p. 3691-3708.
- Winograd, I.J., and Pearson, F.J., Jr., 1976, Major carbon 14 anomaly in a regional carbonate aquifer: Possible evidence for mega scale channeling, south-central Great Basin: *Water Resources Research*, v. 12, No. 6, p. 1125-1143.
- Winograd, I.J., Szabo, B.J., Coplen, T.B., Riggs, A.C., and Kolesar, P.T., 1985, Two-million-year record of deuterium depletion in Great Basin ground waters: *Science*, v. 227, p. 519-522.
- Winograd, I.J., and Thordarson, William, 1968, Structural control of ground-water movement in miogeosynclinal rocks of south-central Nevada, in Eckel, E.B., ed., *Nevada Test Site: Geological Society of America Memoir 110*, p. 35-48.
- , 1975, Hydrogeologic and hydrochemical framework, southcentral Great Basin, Nevada-California, with special reference to the Nevada Test Site: U.S. Geological Survey Professional Paper 712-C, 126 p.